


## Variational and parquet-diagram calculations for neutron matter. IV. Spin-orbit interactions and linear response

E. Krotscheck<sup>1,2</sup> and J. Wang<sup>1</sup>

<sup>1</sup>*Department of Physics, University at Buffalo, SUNY, Buffalo, New York 14260, USA*

<sup>2</sup>*Institut für Theoretische Physik, Johannes Kepler Universität, A-4040 Linz, Austria*

 (Received 23 November 2021; accepted 4 March 2022; published 30 March 2022)

We develop the parquet-diagram summation method for neutron matter interacting via potentials that include spin, tensor, and spin-orbit components. For that purpose, we derive an exact expression for the sum of all ring diagrams in terms of effective local particle-hole interactions involving the above four operators. The parquet equations are closed by deriving the spin-orbit contribution to those particle-hole interactions. We show that many-body correlations screen the bare spin-orbit potential considerably, and the corrections of that screened spin-orbit potential to the other three interaction channels are quite small. We apply our method to the calculation of the response of neutron matter to density and both longitudinal and transverse spin-dependent external fields.

DOI: [10.1103/PhysRevC.105.034345](https://doi.org/10.1103/PhysRevC.105.034345)

### I. INTRODUCTION

#### A. Interactions: Semiempirical nucleon-nucleon forces

Popular models of the nucleon-nucleon forces [1–5] represent the interaction as a sum of local functions times correlation operators, i.e.,

$$\hat{v}(i, j) = \sum_{\alpha=1}^n v_{\alpha}(r_{ij}) \hat{O}_{\alpha}(i, j), \quad (1.1)$$

where  $r_{ij} = |\mathbf{r}_i - \mathbf{r}_j|$  is the distance between particles  $i$  and  $j$ , and the  $\hat{O}_{\alpha}(i, j)$  are operators acting on the spin, isospin, and possibly the relative angular momentum variables of the individual particles. According to the number of operators  $n$ , the potential model is referred to as a  $v_n$  model potential. Semirealistic models for nuclear matter keep at least the six base operators, and these are

$$\begin{aligned} \hat{O}_1(i, j; \hat{\mathbf{r}}_{ij}) &\equiv \hat{O}_c = \mathbb{1}, \\ \hat{O}_3(i, j; \hat{\mathbf{r}}_{ij}) &\equiv \boldsymbol{\sigma}_i \cdot \boldsymbol{\sigma}_j, \\ \hat{O}_5(i, j; \hat{\mathbf{r}}_{ij}) &\equiv S_{ij}(\hat{\mathbf{r}}_{ij}) \equiv 3(\boldsymbol{\sigma}_i \cdot \hat{\mathbf{r}}_{ij})(\boldsymbol{\sigma}_j \cdot \hat{\mathbf{r}}_{ij}) - \boldsymbol{\sigma}_i \cdot \boldsymbol{\sigma}_j, \\ \hat{O}_{2n}(i, j; \hat{\mathbf{r}}_{ij}) &= \hat{O}_{2n-1}(i, j; \hat{\mathbf{r}}_{ij}) \boldsymbol{\tau}_i \cdot \boldsymbol{\tau}_j. \end{aligned} \quad (1.2)$$

where  $\hat{\mathbf{r}}_{ij} = \mathbf{r}_{ij}/r_{ij}$ . We will omit the coordinate arguments when unambiguous.

We have in previous work [6,7] studied  $v_6$  models of the nucleon-nucleon interaction; the next step in the treatment of successively more realistic nucleon-nucleon interactions is the inclusion of the spin-orbit interaction. Its operator structure has the form

$$\begin{aligned} \hat{O}_7(i, j; \mathbf{r}_{ij}, \mathbf{p}_{ij}) &= \mathbf{r}_{ij} \times \mathbf{p}_{ij} \cdot \mathbf{S}, \\ \hat{O}_8(i, j; \mathbf{r}_{ij}, \mathbf{p}_{ij}) &= \hat{O}_7(i, j; \mathbf{r}_{ij}, \mathbf{p}_{ij}) \boldsymbol{\tau}_i \cdot \boldsymbol{\tau}_j, \end{aligned} \quad (1.3)$$

where  $\mathbf{S} \equiv \frac{1}{2}(\boldsymbol{\sigma}_i + \boldsymbol{\sigma}_j)$  is the total spin, and  $\mathbf{p}_{ij} = \frac{1}{2}(\mathbf{p}_i - \mathbf{p}_j)$  is the relative momentum operator of the pair of particles.

This is the subject of the present papers. Unlike the above six operators, the inclusion of spin-orbit interaction in a variational or high-order perturbation theory is much more difficult. Previous studies used partial-wave expansion of plane waves, because partial waves are eigenstates of the spin-orbit operator. This method becomes tedious if one goes to higher-order perturbation theory and has been mostly confined to Bethe-Goldstone calculations [8], three-body coupled cluster [3] calculations, or “low-order constraint variational” (LOCV) [9–11] calculations.

#### B. Methods: Jastrow-Feenberg variational and Parquet diagrams

Diagrammatic perturbation theory is one of the standard methods for dealing with interacting many-body systems. In terms of the paradigms of that method, it is relatively easy to argue what the *minimum* set of Feynman diagrams should be for a reliable microscopic treatment of such systems. Let us, for the purpose of discussion, focus on self-bound systems like  ${}^4\text{He}$ ,  ${}^3\text{He}$ , or nuclear matter. These are characterized by an *equilibrium density* with a negative energy per particle, and *saturation* meaning that the energy per particle will eventually begin to increase with increasing density.

The physical mechanisms behind these effects are clear, as well as the set of Feynman diagrams that need to be included to deal with these effects: At *high density*, saturation is caused by the short-ranged interparticle repulsion. That is dealt with by summing the ladder diagrams, leading to the time-honored Brueckner or Brueckner-Bethe-Goldstone theory [12–17] which has been the workhorse in nuclear theory for decades.

A second important effect is encountered at low densities: As the density is lowered to about  $2/3$  of the saturation density, the system becomes unstable against infinitesimal density fluctuations; this is called the “spinodal point” where the speed of sound goes to zero. In a self-bound Fermi system, a second spinodal point appears at very low density where the interparticle attraction begins to overcome the Pauli pressure. Small fluctuations are dealt with in linear response theory [18,19] which implies, in its simplest version, the calculation of the ring diagrams.

Thus, one is led to the conclusion that the summation of all ring and ladder diagrams of perturbation theory is the least one needs to do for a consistent description of the equation of state of a self-bound many-body system over the whole density regime. This set of diagrams is called the set of “parquet” diagrams. Moreover, the existence of a spinodal point at low density implies that perturbative calculations encounter a divergence.

While the insight into what is needed is quite obvious, the execution is far from trivial. A comprehensive treatment of diagrammatic perturbation theory is found in the seminal paper by Baym and Kadanoff [20], from which it is clear that each two-body vertex depends on 16 variables (2 incoming and 2 outgoing energy/momentum sets). Taking energy and momentum conservation as well as isotropy into account reduces this number to 10, which is still a formidable task. One must seek approximations, but such steps are normally ambiguous without further guidance.

A completely different approach was suggested by Jastrow [21] and Feenberg [22]. For simple, state-independent interactions as appropriate for electrons or quantum fluids, the Jastrow-Feenberg ansatz [22] for the wave function is

$$\Psi_0 = \prod_{\substack{i,j=1 \\ i < j}}^N f(r_{ij}) \Phi_0, \quad (1.4)$$

and its logical generalization to multiparticle correlation functions has been extremely successful. Here  $\Phi_0$  is a model state describing the statistics and, when appropriate, the geometry of the system; for fermions it is normally taken as a Slater determinant, but Bardeen-Cooper-Schrieffer (BCS) states have also been used [23–29].

One of the reasons for the success of this wave function is that it provides a reasonable upper bound for the ground state energy

$$E_0 = \frac{\langle \Psi_0 | H | \Psi_0 \rangle}{\langle \Psi_0 | \Psi_0 \rangle}. \quad (1.5)$$

For that to work the expectation value (1.5) must, of course, be calculated with reasonable accuracy. A particularly useful hierarchy of approximations is the hypernetted-chain summation technique; it is singled out by the fact that it allows, at every level of approximation, the unconstrained optimization of the correlations via the variational principle

$$\frac{\delta E_0}{\delta f}(\mathbf{r}_i, \mathbf{r}_j) = 0. \quad (1.6)$$

In this case, the method is referred to as the (Fermi) Hypernetted-chain Euler-Lagrange [(F)HNC-EL] procedure.

It was quickly realized that the procedure also had exactly the features of high-density saturation and a low-density spinodal instability outlined above. For bosons, Sim, Buchler, and Woo [30] came therefore to the conclusion that “it appears that the optimized Jastrow function is capable of summing all rings and ladders, and partially all other diagrams, to infinite order.” This being more a matter of observation than of physical insight, Jackson, Lande, and Smith went back to diagrammatic perturbation theory and showed in a series of papers [31–33] that indeed the “optimized HNC equations” represented an approximate summation of all parquet diagrams, and determined exactly what these approximations were. With that, a very practical way to perform parquet-diagram summations was found. The types of approximations were singled out by the upper bound property of  $E_0$  as the best possible for the computational price one was willing to pay. Moreover, while the derivation of the relevant equations is somewhat complicated, the resulting equations to be solved numerically were just the Bethe-Goldstone and the random-phase approximation (RPA) equations that had been solved individually for decades.

The above holds, in its rigor, only for bosons. A similar systematic diagrammatic equivalence between the fermion version and parquet-diagram summations has not been carried out. Rather, the equivalence has been highlighted as specific sets of diagrams: rings, ladders, and self-energy insertions [28].

The situation is considerably more complicated for realistic nucleon-nucleon interactions of the form (1.1). A plausible generalization of the wave function (1.4) is the “symmetrized operator product” [34,35]

$$\Psi_0^{\text{SOP}} = \mathcal{S} \left[ \prod_{\substack{i,j=1 \\ i < j}}^N \hat{f}(i, j) \right] \Phi_0, \quad (1.7)$$

where

$$\hat{f}(i, j) = \sum_{\alpha=1}^n f_{\alpha}(r_{ij}) \hat{O}_{\alpha}(i, j), \quad (1.8)$$

and  $\mathcal{S}$  stands for symmetrization. The symmetrization is necessary because the operators  $\hat{O}_{\alpha}(i, j)$  and  $\hat{O}_{\beta}(i, k)$  do not necessarily commute. We have highlighted recently [7] (see also Ref. [36]) the importance of a proper symmetrization in cases where the bare interaction is different in spin-singlet and spin-triplet channels. As an extreme case, some commutator diagrams would *diverge* for hard-core interactions if the correlation functions  $f_{\alpha}(r_{ij})$  were determined by some simplistic method like LOCV. Due to the complications of a fully symmetrized variational wave functions, only very simple implementations were introduced, like omitting commutators altogether [34] or treating that state-dependent correlations in a simple chain approximation (single operator chains, SOC) [35].

Light was shed on the meaning of commutator corrections again from the point of view of parquet-diagram summations. Smith and Jackson [37] showed for a fictitious system of

bosons with spin, isospin, and tensor forces that the parquet-diagram summation led to no commutator diagrams, i.e., to an optimized Bose-version of Ref. [34].

The conclusion is therefore that, unlike originally believed, the optimized variational wave function (1.7) contains more than just the parquet set; nonparquet diagrams simply are neglected when commutators are neglected. This does not solve the problem that these corrections are potentially important. Again, within naïve perturbation theory, the computation of these diagrams is extremely cumbersome. We have therefore taken in Ref. [7] a hybrid approach and included the leading nonparquet diagrams in a local approximation suggested by the variational wave function (1.7)(1.8). As expected, rather significant changes in the short-ranged structure of correlations and effective interactions were found.

This paper is devoted to the next step towards including realistic nucleon-nucleon interactions by dealing with spin-orbit forces. The diagrammatic task is somewhat easier than including “nonparquet” diagrams because the spin-orbit force acts only in spin-triplet states. On the other hand it is made much more complicated since neither the “chaining” (as in the summation of ring diagrams) nor the parallel connection (as in the summation of the ladder diagrams) of two spin-orbit operators generates another spin-orbit operator. We shall propose very specific approximate schemes that are, again, inspired by the Jastrow-Feenberg theory.

## II. VARIATIONAL AND PARQUET-DIAGRAM THEORY FOR SPIN-ORBIT FORCES

### A. Chain diagrams

#### 1. Chain-diagram summation of spins and tensors

Let us as an introductory exercise briefly review the summation of chain diagrams for an interaction of the  $V_6$  form [6]. We assume a *local* effective particle-hole interaction

$$\hat{V}_{p-h}(q) = \sum_{\alpha=1}^6 \tilde{V}_{p-h}^{(\alpha)}(q) \hat{O}_{\alpha}(i, j), \quad (2.1)$$

which is given in momentum space. Note that this is not the bare interaction, and also *not* directly related to the  $G$  matrix of Brueckner theory but rather, in the long-wavelength limit, to Landau’s Fermi-liquid theory [38–40] or, at finite wave numbers, to pseudopotentials [41]. In neutron matter, the operators are projected to the isospin = 1 channel and the above sum goes over the odd values of  $\alpha$  only. As usual, we define the Fourier transforms with a density factor, i.e.,

$$\tilde{V}_{p-h}^{(\alpha)}(q) = \begin{cases} \rho \int d^3r V_{p-h}^{(\alpha)}(r) j_0(qr) & \text{for } \alpha = 1, \dots, 3, \\ -\rho \int d^3r V_{p-h}^{(\alpha)}(r) j_2(qr) & \text{for } \alpha = 5. \end{cases} \quad (2.2)$$

For further reference we define

$$\chi_0(\mathbf{q}, \mathbf{h}; \omega) = -\frac{1}{\varepsilon_p - \varepsilon_h - \hbar\omega - i\eta} - \frac{1}{\varepsilon_p - \varepsilon_h + \hbar\omega + i\eta}. \quad (2.3)$$

Then, the response function of the noninteracting Fermi fluid is the hole-state average  $(1/N) \sum_{\mathbf{h}}$  of  $\chi_0(q, \mathbf{h}; \omega)$  with the

corresponding spin trace  $\text{Tr}_{\sigma}$ :

$$\chi_0(q; \omega) = \frac{1}{N} \text{Tr}_{\sigma} \sum_{\mathbf{h}} \chi_0(q, \mathbf{h}; \omega). \quad (2.4)$$

As a convention, we will label occupied (“hole”) states by  $\mathbf{h}$ ,  $\mathbf{h}'$ ,  $\mathbf{h}_i$  and unoccupied (“particle”) states by  $\mathbf{p}$ ,  $\mathbf{p}'$ ,  $\mathbf{p}_i$ ; labels  $\mathbf{q}$ ,  $\mathbf{q}'$ , and  $\mathbf{q}_i$  are used here to represent the particle-hole-transition wave number, i.e., we always assume  $\mathbf{p}_i = \mathbf{h}_i + \mathbf{q}_i$  if there is no ambiguity.

We begin with the chain approximation of the effective interaction

$$\hat{W}(\mathbf{q}; \omega) = \hat{V}_{p-h}(\mathbf{q}) + [\hat{V}_{p-h} * \chi_0(q; \omega) * \hat{V}_{p-h}] + \dots \quad (2.5)$$

and the induced interaction

$$\hat{w}_1(\mathbf{q}; \omega) = \hat{W}(\mathbf{q}; \omega) - \hat{V}_{p-h}(\mathbf{q}; \omega). \quad (2.6)$$

Above we have defined the convolution product of two operators  $\hat{A} \equiv \hat{A}(\mathbf{q}, \mathbf{h}, \mathbf{h}', \sigma, \sigma')$  and  $\hat{B} \equiv \hat{B}(\mathbf{q}, \mathbf{h}, \mathbf{h}', \sigma, \sigma')$  as

$$\begin{aligned} [\hat{A} * \chi_0 * \hat{B}](\mathbf{q}, \mathbf{h}, \mathbf{h}', \sigma, \sigma') \\ = \frac{1}{N} \text{Tr}_{\sigma''} \sum_{\mathbf{h}''} \hat{A}(\mathbf{q}, \mathbf{h}, \mathbf{h}'', \sigma, \sigma'') \chi_0(\mathbf{q}, \mathbf{h}''; \omega) \\ \times \hat{B}(\mathbf{q}, \mathbf{h}'', \mathbf{h}', \sigma'', \sigma'). \end{aligned} \quad (2.7)$$

To carry out the summation of chain diagrams, it is convenient to transform the spin and tensor operators into the longitudinal and transverse operators [42,43]

$$\hat{Q}_1 \equiv \mathbb{1}, \quad (2.8a)$$

$$\hat{Q}_3 \equiv \hat{L}(\hat{\mathbf{q}}) = (\boldsymbol{\sigma} \cdot \hat{\mathbf{q}})(\boldsymbol{\sigma}' \cdot \hat{\mathbf{q}}), \quad (2.8b)$$

$$\hat{Q}_5 \equiv \hat{T}(\hat{\mathbf{q}}) = \boldsymbol{\sigma} \cdot \boldsymbol{\sigma}' - (\boldsymbol{\sigma} \cdot \hat{\mathbf{q}})(\boldsymbol{\sigma}' \cdot \hat{\mathbf{q}}). \quad (2.8c)$$

In the basis  $\hat{Q}_{\alpha} \in \{\mathbb{1}, \hat{L}, \hat{T}\} \times \{\mathbb{1}, \tau_1 \cdot \tau_2\}$ , the convolution product (2.7) decouples in the individual channels. The effective interactions (2.5) and (2.6) can then be written as

$$\hat{W}(\mathbf{q}; \omega) = \sum_{\alpha=1}^6 \tilde{W}^{(\alpha)}(q; \omega) \hat{Q}_{\alpha}, \quad (2.9)$$

with

$$\tilde{W}^{(\alpha)}(q; \omega) = \frac{\tilde{V}_{p-h}^{(\alpha)}(q)}{1 - \tilde{V}_{p-h}^{(\alpha)}(q) \chi_0(q; \omega)}. \quad (2.10)$$

and, correspondingly,  $\hat{w}_1(\mathbf{q}; \omega)$ . Thus, the summation of chain diagrams is straightforward in the first six (or three) operator channels.

#### 2. Chain-diagram summation in the spin-orbit channel

The task is more complex for spin-orbit-like interactions since the different channels cannot be decoupled. First, we note that it is an *assumption* that the particle-hole interaction can be written in the simple form  $V_{p-h}^{(LS)}(r) \mathbf{L} \cdot \mathbf{S}$ : Even the  $G$  matrix includes, for a bare spin-orbit force, powers of the angular momentum operator to all orders. That has, so far, precluded the extension of manifestly microscopic approaches for spin-orbit forces to the parquet level. This assumption has, nevertheless, been quite popular in particular in connection

with the study of the nuclear response using Skyrme interactions [44–52].

Since we will frequently need the wave vectors  $\mathbf{h}$ ,  $\mathbf{h}'$ , ... in units of the Fermi wave number  $k_F$ , we also abbreviate  $\mathbf{h}_F \equiv \mathbf{h}/k_F$ . Also, let  $\Delta\mathbf{h} \equiv \mathbf{h} - \mathbf{h}'$  and define correspondingly  $\Delta\mathbf{h}_F \equiv \Delta\mathbf{h}/k_F$ . The spatial matrix elements of the spin-orbit interaction are then

$$\begin{aligned} & \langle \mathbf{h} + \mathbf{q}, \mathbf{h}' | V_{p-h}^{(LS)}(r) \mathbf{L} \cdot \mathbf{S} | \mathbf{h}, \mathbf{h}' + \mathbf{q} \rangle \\ &= \frac{1}{N} \tilde{V}_{p-h}^{(LS)}(q) i\hat{\mathbf{q}} \times \Delta\mathbf{h}_F \cdot \mathbf{S} \equiv \frac{1}{N} \tilde{V}_{p-h}^{(LS)}(q) \widetilde{\mathbf{L}} \cdot \mathbf{S}, \end{aligned} \quad (2.11a)$$

$$\begin{aligned} & \langle \mathbf{h} + \mathbf{q}, \mathbf{h}' - \mathbf{q} | V_{p-h}^{(LS)}(r) \mathbf{L} \cdot \mathbf{S} | \mathbf{h}, \mathbf{h}' \rangle \\ &= \frac{1}{N} \tilde{V}_{p-h}^{(LS)}(q) i\hat{\mathbf{q}} \times \Delta\mathbf{h}_F \cdot \mathbf{S} \equiv \frac{1}{N} \tilde{V}_{p-h}^{(LS)}(q) \widetilde{\mathbf{L}} \cdot \mathbf{S} \end{aligned} \quad (2.11b)$$

with

$$\tilde{V}_{p-h}^{(LS)}(q) = \frac{\rho}{2} \int d^3r V_{p-h}^{(LS)}(r) r k_F j_1(qr), \quad (2.12)$$

$$\widetilde{\mathbf{L}} \cdot \mathbf{S} = i\hat{\mathbf{q}} \times \Delta\mathbf{h}_F \cdot \mathbf{S}. \quad (2.13)$$

From here on, we shall generally mean the *momentum space* representations (2.8), (2.13) when we refer to the operators  $\hat{O}_\alpha$ ,  $\hat{Q}_\alpha$  or  $\widetilde{\mathbf{L}} \cdot \mathbf{S}$ . Note in particular that the operator  $\widetilde{\mathbf{L}} \cdot \mathbf{S}$  acts only in spin-space and depends parametrically on the direction  $\hat{\mathbf{q}}$  of momentum transfer and the difference of the hole wave numbers  $\Delta\mathbf{h}$ .

$\tilde{V}_{p-h}^{(LS)}(q)$  is defined such that its dimensions are the same in both coordinate and momentum space. Note also that we have defined the operator  $\widetilde{\mathbf{L}} \cdot \mathbf{S}$  as dimensionless; as a consequence  $\tilde{V}_{p-h}^{(LS)}(q)$  has the dimension of an energy.

The manipulations to derive an effective interaction including a spin-orbit potential are rather involved; they will be presented in Appendix A where we will derive a closed-form expression for the effective interaction (2.5). We focus on the spin channels of the operator set. Besides the operators  $\hat{Q}_1$ ,  $\hat{Q}_3$ , and  $\hat{Q}_5$ , we need to define three additional operators

$$\hat{Q}_7 \equiv [(\hat{\mathbf{q}} \times \mathbf{h}_F) \cdot \boldsymbol{\sigma}] [(\hat{\mathbf{q}} \times \mathbf{h}'_F) \cdot \boldsymbol{\sigma}'], \quad (2.14a)$$

$$\hat{Q}_9 \equiv 2(\hat{\mathbf{q}} \times \mathbf{h}_F) \cdot (\hat{\mathbf{q}} \times \mathbf{h}'_F), \quad (2.14b)$$

and

$$\widetilde{\mathbf{L}} \mathbf{S}' \equiv \frac{i}{2} [(\hat{\mathbf{q}} \times \mathbf{h}_F) \cdot \boldsymbol{\sigma} - (\hat{\mathbf{q}} \times \mathbf{h}'_F) \cdot \boldsymbol{\sigma}']. \quad (2.14c)$$

The corresponding channels with isospin operators  $\tau_1 \cdot \tau_2$  will follow exactly the same algebra.

The set of operators  $\{\hat{Q}_\alpha\}$  has the properties

$$[\hat{Q}_\alpha * \chi_0 * \hat{Q}_\beta] = \begin{cases} \chi_0(q; \omega) \hat{Q}_\alpha \delta_{\alpha\beta} & \text{for } \alpha = 1, 3, 5, \\ \chi_0^{(\perp)}(q; \omega) \hat{Q}_\alpha \delta_{\alpha\beta} & \text{for } \alpha = 7, 9 \end{cases} \quad (2.15)$$

with the “transverse” Lindhard function

$$\chi_0^{(\perp)}(q; \omega) = \frac{1}{N} \text{Tr}_\sigma \sum_{\mathbf{h}} |\hat{\mathbf{q}} \times \mathbf{h}_F|^2 \chi_0(\mathbf{q}, \mathbf{h}; \omega). \quad (2.16)$$

The explicit form of  $\chi_0^{(\perp)}(q; \omega)$  is given in Appendix B.

In terms of these operators, the effective interaction consists of two contributions: one that contains only even powers

of the spin-orbit interaction and one that contains odd powers. For a compact representation, we define *energy-dependent* “particle-hole” interactions in the central and the transverse channels,

$$\tilde{V}_{p-h}^{(c)}(q; \omega) \equiv \tilde{V}_{p-h}^{(c)}(q) + \frac{1}{4} \chi_0^{(\perp)}(q; \omega) [\tilde{V}_{p-h}^{(LS)}(q)]^2, \quad (2.17a)$$

$$\tilde{V}_{p-h}^{(T)}(q; \omega) \equiv \tilde{V}_{p-h}^{(T)}(q) + \frac{1}{8} \chi_0^{(\perp)}(q; \omega) [\tilde{V}_{p-h}^{(LS)}(q)]^2. \quad (2.17b)$$

There is no energy-dependent correction to the longitudinal channel; we nevertheless define, for a symmetric notation,  $\tilde{V}_{p-h}^{(L)}(q; \omega) \equiv \tilde{V}_{p-h}^{(L)}(q)$ . The effective interactions for  $\alpha = 1, \dots, 9$  can contain only even numbers of spin-orbit operators; we can write it as

$$\hat{W}^{(\text{even})}(\mathbf{q}, \mathbf{h}, \mathbf{h}', \boldsymbol{\sigma}, \boldsymbol{\sigma}'; \omega) = \sum_{\alpha \text{ odd}}^9 \tilde{W}^{(\alpha)}(q; \omega) \hat{Q}_\alpha \quad (2.18)$$

with

$$\tilde{W}^{(\alpha)}(q; \omega) = \frac{\tilde{V}_{p-h}^{(\alpha)}(q; \omega)}{1 - \chi_0(q; \omega) \tilde{V}_{p-h}^{(\alpha)}(q; \omega)} \quad (2.19)$$

for  $\alpha = 1, \dots, 5$  and

$$\tilde{W}^{(7)}(q; \omega) = \frac{1}{4} \frac{[\tilde{V}_{p-h}^{(LS)}(q)]^2 \chi_0(q; \omega)}{1 - \chi_0(q; \omega) \tilde{V}_{p-h}^{(c)}(q; \omega)}, \quad (2.20)$$

$$\tilde{W}^{(9)}(q; \omega) = \frac{1}{8} \frac{[\tilde{V}_{p-h}^{(LS)}(q)]^2 \chi_0(q; \omega)}{1 - \chi_0(q; \omega) \tilde{V}_{p-h}^{(T)}(q; \omega)}. \quad (2.21)$$

For odd numbers of spin-orbit operators we get

$$\begin{aligned} & \hat{W}_{LS}^{(\text{odd})}(\mathbf{q}, \mathbf{h}, \mathbf{h}', \boldsymbol{\sigma}, \boldsymbol{\sigma}'; \omega) \\ &= \frac{\tilde{V}_{p-h}^{(LS)}(q)}{1 - \chi_0(q; \omega) \tilde{V}_{p-h}^{(c)}(q; \omega)} [\widetilde{\mathbf{L}} \cdot \mathbf{S} - \widetilde{\mathbf{L}} \mathbf{S}'] \\ &+ \frac{\tilde{V}_{p-h}^{(LS)}(q)}{1 - \chi_0(q; \omega) \tilde{V}_{p-h}^{(T)}(q; \omega)} \widetilde{\mathbf{L}} \mathbf{S}' \\ &\equiv \tilde{W}_{LS}^{(LS)}(q; \omega) \widetilde{\mathbf{L}} \cdot \mathbf{S} + \tilde{W}_{LS}^{(LS')} (q; \omega) \widetilde{\mathbf{L}} \mathbf{S}'. \end{aligned} \quad (2.22)$$

### 3. Response functions

The response functions describe the response of a system to an external perturbation. In our case, the external fields may be a scalar field or a longitudinal and transverse spin-dependent field [53,54],

$$h_{\text{ext}}^{(c)}(\mathbf{q}), \quad h_{\text{ext}}^{(L)}(\mathbf{q}) \hat{\mathbf{q}} \cdot \boldsymbol{\sigma}, \quad \text{and} \quad h_{\text{ext}}^{(T)}(\mathbf{q}) (\hat{\mathbf{q}} \times \boldsymbol{\sigma}). \quad (2.23)$$

The simplest approximation to the (spin-)density response function  $\chi(q; \omega)$  is the random-phase approximation (RPA) [55,56], which implies the summation of chain diagrams as carried out above. One can go beyond that by including two-particle–two-hole states in the excitation operator [57–61]; the procedure is known as second RPA (SRPA) in nuclear physics. When built upon a correlated ground state, the method has been termed dynamic many-body theory (DMBT) and has led to unprecedented agreement between experiments and theories for the helium liquids [62–66]. These complications are

expected to be much less important in neutron matter due to its lower density.

In the RPA, the response to the three external fields (2.23) (plus possible isospin components) is

$$\begin{aligned}\chi_\alpha(q, \omega) &= \frac{\chi_0(q, \omega)}{1 - \tilde{V}_{\text{p-h}}^{(\alpha)}(q, \omega)\chi_0(q, \omega)} \\ &= \chi_0(q, \omega) + \chi_0(q, \omega)\tilde{W}^{(\alpha)}(q, \omega)\chi_0(q, \omega)\end{aligned}\quad (2.24)$$

for  $\alpha = 1, \dots, 5$ , where the  $\tilde{V}_{\text{p-h}}^{(\alpha)}(q, \omega)$  contain, in our case, the energy-dependent corrections (2.17a) and (2.17b) originating from the spin-orbit potential.

We are not aware of external fields that couple directly to the hole momenta and thus would probe directly the components  $\tilde{W}^{(7)}(q, \omega)$ ,  $\tilde{W}^{(9)}(q, \omega)$ , and the spin-orbit components of the effective interaction.

#### 4. Local approximation

The derivation was so far exact in the sense that we have only assumed that the particle-hole irreducible interaction  $\hat{V}_{\text{p-h}}(\mathbf{q})$  can be written in the form of a  $v_8$  potential. As we can see, the total effective interaction *cannot* be represented in a  $v_8$  form, but we were able to derive a closed form in terms of a small number of operators. The exact form derived above would certainly be useful for the study of  $P$ -wave pairing in neutron matter where a very accurate representation of the effective interaction at the Fermi surface is needed.

This is not the purpose of the present work; rather we seek an optimal approximation of the interaction in a  $v_8$  form for the purpose of a complete summation of the parquet class of diagrams. Following and generalizing the procedure defined in the parquet-diagram papers [6,31,32,37], we define

the local approximations for all quantities by calculating the hole-state average

$$\tilde{W}^{(\alpha)}(q) = \frac{\text{Tr}_{\sigma\sigma'} \int \frac{d^3h d^3h'}{V_F^2} \hat{W}(\mathbf{q}, \mathbf{h}, \mathbf{h}') \hat{Q}_\alpha(\mathbf{q})}{\text{Tr}_{\sigma\sigma'} \langle \hat{Q}_\alpha^2 \rangle}, \quad (2.25)$$

where  $V_F = 4\pi k_F^3/3$  is the volume of the Fermi sphere, and it is assumed that the effective interaction is written in the form (2.9). For the first six operators, the hole-state integration is trivial, and Eq. (2.25) reduces to

$$\tilde{W}^{(\alpha)}(q) = \frac{\text{Tr}_{\sigma\sigma'} \hat{O}_\alpha(\hat{\mathbf{q}}) \hat{W}(\mathbf{q}, \mathbf{h}, \mathbf{h}')}{\text{Tr}_{\sigma\sigma'} \hat{O}_\alpha^2(\hat{\mathbf{q}})}. \quad (2.26)$$

The spin-orbit term can be done similarly: For a local interaction in  $v_8$  form we get

$$\begin{aligned}\frac{1}{\nu^2} \text{Tr}_{\sigma\sigma'} \int \frac{d^3h d^3h'}{V_F^2} \hat{W}(\mathbf{q})(-i\hat{\mathbf{q}} \times \Delta\mathbf{h}_F) \cdot \mathbf{S} \\ = \frac{1}{\nu^2} \tilde{W}^{(\text{LS})}(q) \text{Tr}_{\sigma\sigma'} \int \frac{d^3h d^3h'}{V_F^2} [(\hat{\mathbf{q}} \times \Delta\mathbf{h}_F) \cdot \mathbf{S}]^2 \\ = \frac{1}{2} \tilde{W}^{(\text{LS})}(q) \int \frac{d^3h d^3h'}{V_F^2} |\hat{\mathbf{q}} \times \Delta\mathbf{h}_F|^2 = \frac{2}{5} \tilde{W}^{(\text{LS})}(q),\end{aligned}\quad (2.27)$$

where  $\nu$  is the degree of degeneracy of single-particle states.

With that we can derive a local approximation for the full effective interaction (2.10) in the  $v_8$  (or  $v_4$ ) form. The trace (2.27) with the components  $\tilde{W}^{(7)}(q; \omega)$  and  $\tilde{W}^{(9)}(q; \omega)$  is zero. The only nontrivial quantity is  $\tilde{W}^{(\text{LS})}(q; \omega)$ , for which we obtain

$$\begin{aligned}\frac{5}{2\nu^2} \text{Tr}_{\sigma\sigma'} \int \frac{d^3h d^3h'}{V_F^2} \tilde{W}^{(\text{LS}')}(q; \omega) \tilde{\mathbf{L}}\tilde{\mathbf{S}}'[-i\hat{\mathbf{q}} \times (\mathbf{h}_F - \mathbf{h}'_F)] \cdot \mathbf{S} \\ = \frac{5}{8\nu^2} \tilde{W}^{(\text{LS}')}(q; \omega) \text{Tr}_{\sigma\sigma'} \int \frac{d^3h d^3h'}{V_F^2} [(\hat{\mathbf{q}} \times \mathbf{h}_F) \cdot \boldsymbol{\sigma} - (\hat{\mathbf{q}} \times \mathbf{h}'_F) \cdot \boldsymbol{\sigma}'] [(\hat{\mathbf{q}} \times (\mathbf{h}_F - \mathbf{h}'_F)) \cdot (\boldsymbol{\sigma} + \boldsymbol{\sigma}')] \\ = \frac{1}{2} \tilde{W}^{(\text{LS}')}(q; \omega)\end{aligned}\quad (2.28)$$

such that the localized effective spin-orbit interaction is simply

$$\begin{aligned}\tilde{W}_{\text{local}}^{(\text{LS})}(q; \omega) &= \tilde{W}^{(\text{LS})}(q, \omega) + \frac{1}{2} \tilde{W}^{(\text{LS}')}(q, \omega) \\ &= \frac{1}{2} \frac{\tilde{V}_{\text{p-h}}^{(\text{LS})}(q)}{1 - \chi_0(q; \omega)\tilde{V}_{\text{p-h}}^{(\text{c})}(q; \omega)} \\ &\quad + \frac{1}{2} \frac{\tilde{V}_{\text{p-h}}^{(\text{LS})}(q)}{1 - \chi_0(q; \omega)\tilde{V}_{\text{p-h}}^{(\text{T})}(q; \omega)}.\end{aligned}\quad (2.29)$$

With that, we have defined a reasonably compact form of the effective interaction  $\hat{W}_{\text{local}}(\mathbf{q}; \omega)$  in the  $v_8$  form. Since we will

not use the nonlocal version in our further considerations we shall henceforth omit the subscript ‘‘local’’.

The practical implementation of a full parquet-level calculation requires yet another step. Above, we defined a local but energy-dependent effective interaction. To define a static effective interaction, we follow the procedure outlined in Refs. [31,32] and generalized to fermions in Ref. [6,28]:

- (1) Assume a static effective particle-hole interaction  $\hat{V}_{\text{p-h}}(\mathbf{q})$ . Calculate the density–density response function, which we can write as

$$\chi_\alpha(q, \omega) = \chi_0(q, \omega) + \chi_0(q, \omega)\tilde{W}^{(\alpha)}(q, \omega)\chi_0(q, \omega), \quad (2.30)$$

and, from that, the static structure functions  $S_\alpha(q)$

$$S_\alpha(q) = - \int \frac{d\omega}{\pi} \text{Im} \chi_\alpha(q, \omega). \quad (2.31)$$

(2) Define a *static* effective interaction such that the second-order response function

$$\chi_\alpha(q, \omega) = \chi_0(q, \omega) + \chi_0(q, \omega) \tilde{W}^{(\omega)}(q) \chi_0(q, \omega) \quad (2.32)$$

leads to the same  $S(q)$ . Combining the two relationships, we can define an energy independent effective interaction as

$$\tilde{W}^{(\omega)}(q) = \frac{\int \frac{d\omega}{\pi} \text{Im} \chi_0(q, \omega) \tilde{W}^{(\omega)}(q, \omega) \chi_0(q, \omega)}{\int \frac{d\omega}{\pi} \text{Im} \chi_0^2(q, \omega)}. \quad (2.33)$$

We use the same procedure to define an energy-independent interaction in the spin-orbit channel. We stress, of course, that the dynamic interaction  $\hat{W}(\mathbf{q}, \omega)$  is replaced by the static  $\hat{W}(\mathbf{q})$  only for the ground state correlations. In both the calculation of the dynamic structure function, to be discussed below, as well as in the calculation of pairing phenomena [28,29] we keep the full energy dependence.

### B. Particle-hole potential with spin-orbit interactions

For bosons, the situation is very simple: One ends up, up to an undetermined function  $V_1(r)$ , with exactly the HNC-EL equations or the “localized parquet” equations [32,33]. The correction  $V_1(r)$  is identified, in Jastrow-Feenberg theory, with the contribution from “elementary diagrams” and multiparticle correlations. In the language of parquet theory it stems from totally irreducible diagrams [67].

The situation is somewhat more complicated for fermions due to the multitude of exchange contributions. The RPA form (2.5) specifies that one keeps only the simplest exchange loops. The relevant approximations have been dubbed FHNC//0 or parquet//0. More complicated exchange diagrams are also important and routinely kept [6,7] but we shall restrict ourselves for the purpose of discussions to the simplest case. A brief discussion of how we include exchange effects will be given in Sec. II D.

We take here a similarly pragmatic approach as the one behind Jastrow-Feenberg theory: Rather than calculating some low-order contributions to high precision and then getting stuck doing high-order terms, we use local approximations of the kind suggested by the Jastrow-Feenberg wave function for those terms that are otherwise omitted. In this case, the effective interaction  $\hat{V}_{\text{p-h}}(\mathbf{q})$  is structurally identical to that for bosons, i.e.,

$$V_{\text{p-h}}(r) = \frac{\hbar^2}{m} |\nabla \sqrt{1 + \Gamma_{\text{dd}}(r)}|^2 + [1 + \Gamma_{\text{dd}}(r)]v(r) + \Gamma_{\text{dd}}(r)w_1(r). \quad (2.34)$$

Here,  $\Gamma_{\text{dd}}(r)$  is the direct correlation function. This function is rigorously defined as the sum of all “direct-direct” diagrams of the FHNC diagrammatic summation method [68,69]. In the simplest FHNC//0 or parquet//0 approximation, it is related

to the density static structure function by

$$\tilde{\Gamma}_{\text{dd}}(q) = \frac{S_{\text{F}}(q) - S(q)}{S_{\text{F}}^2(q)}. \quad (2.35)$$

The induced interaction  $w_1(r; \omega)$  defined in Eq. (2.6) is approximated by a local function  $w_1(r)$  by the same procedure that was used to define an energy-independent effective interaction, i.e., we simply have

$$w_1(r) = W(r) - V_{\text{p-h}}(r). \quad (2.36)$$

Beginning with  $v_6$  interactions, the correlation functions become angle dependent. The expression (2.34) becomes

$$\hat{V}_{\text{p-h}}(\mathbf{r}) = \frac{\hbar}{m} |\nabla \psi(\mathbf{r})|^2 + \psi^*(\mathbf{r})[\hat{V}(r) + \hat{V}_I(\mathbf{r}) + \hat{w}_I(\mathbf{r})]\psi(\mathbf{r}) - \hat{w}_I(\mathbf{r}), \quad (2.37)$$

where we have omitted all spin (and possibly isospin) dependencies for ease of writing. The  $\hat{V}_I(\mathbf{r})$  is in our case the important contribution of “twisted-chain” diagrams [7].

The pair wave functions  $\psi(\mathbf{r})$  are related to the direct correlation functions by

$$|\psi(\mathbf{r})|^2 = 1 + \Gamma_{\text{dd}}(r). \quad (2.38)$$

The short-ranged structure of the pair wave function  $\psi(\mathbf{r})$  is determined by a Bethe-Goldstone-like equation [28],

$$\psi^*(\mathbf{r}) \left[ -\frac{\hbar^2}{2m} \nabla^2 + \hat{v}(\mathbf{r}) + \hat{V}_I(\mathbf{r}) + \hat{w}_I(\mathbf{r}) \right] \psi(\mathbf{r}) = [t(k)[1 - S_{\text{F}}^{-1}(k)]\hat{\Gamma}_{\text{dd}}(k)]^{\mathcal{F}}(r). \quad (2.39)$$

Alternatively [9–11,70,71] the short-ranged structure has been determined by an effective Schrödinger equation supplemented by a “healing” condition (LOCV method).

In the case of  $v_6$  model interactions, the products of wave functions and potentials decouple in the projector channels  $\hat{P}_\alpha \in \{\hat{P}_s, \hat{P}_{t+}, \hat{P}_{t-}\}$ . The only new aspect is that we must keep the angular dependence of the tensor correlations in the kinetic energy term  $|\nabla \psi(\mathbf{r})|^2$  in Eq. (2.37). We have described this in Ref. [6]; see also Ref. [37].

The situation becomes again more complicated if spin-orbit components are included. There are two origins of a spin-orbit contributions to the particle-hole interaction: One comes from the terms

$$\psi^*(\mathbf{r})v_{\text{LS}}(r)\mathbf{L}\cdot\mathbf{S}\psi(\mathbf{r})$$

and

$$\psi^*(\mathbf{r})w_1^{(\text{LS})}(r)\mathbf{L}\cdot\mathbf{S}\psi(\mathbf{r}) - w_1^{(\text{LS})}(r)\mathbf{L}\cdot\mathbf{S}.$$

The spin-orbit operator commutes with a spherically symmetric wave function, hence we can write this term as

$$V_{\text{p-h}}^{(\text{LS})}(r) = [v_{\text{LS}}(r)[1 + \Gamma_{\text{dd}}(r)] + w_1^{(\text{LS})}(r)\Gamma_{\text{dd}}(r)]. \quad (2.40)$$

A second contribution to the particle-hole interaction in spin-orbit channel comes from the modification of the wave function due to a spin-orbit term in Eq. (2.39). That correction goes to zero for both  $r \rightarrow 0$  and  $r \rightarrow \infty$  [9,71]. Considering the fact that, as we shall see, the spin-orbit corrections are

small anyway, we follow here the strategy of Ref. [71] and disregard this term. As already mentioned above, we can also safely disregard the “twisted-chain” corrections [7]. These corrections are important when the interactions in the spin-singlet and the spin-triplet cases are very different, as is the case for both the Reid [1] and the Argonne [4] potentials. The

spin-orbit force acts only in spin-triplet channels, one does therefore not expect significant corrections from nonparquet contributions.

### C. Energy correction

Let us first look at the direct part of the second-order correction to the energy,

$$\Delta E_2 = -\frac{N^3}{2} \sum_{\sigma_p \sigma_{p'} \sigma_h \sigma_{h'}} \int \frac{d^3 q d^3 h d^3 h'}{(2\pi)^9 \rho^3} \frac{|\langle \mathbf{h} + \mathbf{q} \sigma_p, \mathbf{h}' - \mathbf{q} \sigma_{p'} | \hat{v} | \mathbf{h} \sigma_h, \mathbf{h}' \sigma_{h'} \rangle|^2}{e_p + e_{p'} - e_h - e_{h'}}. \quad (2.41)$$

Focusing on the spin-orbit contribution, we get from (2.11b)

$$\langle \mathbf{h} + \mathbf{q} \sigma_p, \mathbf{h}' - \mathbf{q} \sigma_{p'} | v_{\text{LS}}(r) \mathbf{L} \cdot \mathbf{S} | \mathbf{h} \sigma_h, \mathbf{h}' \sigma_{h'} \rangle = \frac{1}{N} \tilde{V}_{\text{LS}}(q) \langle \sigma_p \sigma_{p'} | \widetilde{\mathbf{L}} \cdot \mathbf{S} | \sigma_h \sigma_{h'} \rangle \quad (2.42)$$

and for the energy correction

$$\frac{\Delta E_2}{N} = -\frac{1}{2} \int \frac{d^3 q}{(2\pi)^3 \rho} \tilde{v}_{\text{LS}}^2(q) \int \frac{d^3 h d^3 h'}{(2\pi)^6 \rho^2} \sum_{\sigma_p \sigma_{p'} \sigma_h \sigma_{h'}} \frac{|\langle \sigma_p \sigma_{p'} | \widetilde{\mathbf{L}} \cdot \mathbf{S} | \sigma_h \sigma_{h'} \rangle|^2}{e_p + e_{p'} - e_h - e_{h'}}. \quad (2.43)$$

The matrix element of the spin-orbit operators evaluate to

$$\sum_{\sigma_p \sigma_{p'} \sigma_h \sigma_{h'}} |\langle \sigma_p \sigma_{p'} | \widetilde{\mathbf{L}} \cdot \mathbf{S} | \sigma_h \sigma_{h'} \rangle|^2 = \text{Tr}_{\sigma_p \sigma_{p'}} (\hat{\mathbf{q}} \times \Delta \mathbf{h}_F \cdot \mathbf{S})^2 = \frac{v^2}{2} |\hat{\mathbf{q}} \times \Delta \mathbf{h}_F|^2$$

such that

$$\frac{\Delta E_2}{N} = -\frac{1}{4} \int \frac{d^3 q}{(2\pi)^3 \rho} \tilde{v}_{\text{LS}}^2(q) \int \frac{d^3 h d^3 h'}{V_F^2} \frac{|\hat{\mathbf{q}} \times \Delta \mathbf{h}_F|^2}{e_p + e_{p'} - e_h - e_{h'}}. \quad (2.44)$$

To go higher orders, use [72]

$$\int_0^\infty \frac{d\omega}{\pi} \text{Im} \chi_0(\mathbf{q}, \mathbf{h}; \omega) \chi_0(-\mathbf{q}, \mathbf{h}'; \omega) = \frac{1}{e_p + e_{p'} - e_h - e_{h'}}. \quad (2.45)$$

In our specific case we get

$$\begin{aligned} \int \frac{d^3 h d^3 h'}{V_F^2} \frac{|\hat{\mathbf{q}} \times \Delta \mathbf{h}_F|^2}{e_p + e_{p'} - e_h - e_{h'}} &= 2 \int_0^\infty \frac{d\omega}{\pi} \text{Im} \int \frac{d^3 h d^3 h'}{V_F^2} |\hat{\mathbf{q}} \times \Delta \mathbf{h}_F|^2 \chi_0(\mathbf{q}, \mathbf{h}; \omega) \chi_0(-\mathbf{q}, \mathbf{h}'; \omega) \\ &= 4 \int_0^\infty \frac{d\omega}{\pi} \text{Im} \chi_0(q; \omega) \chi_0^{(\perp)}(q, \omega) \end{aligned} \quad (2.46)$$

and with that

$$\frac{\Delta E_2}{N} = -\frac{1}{2} \int \frac{d^3 q}{(2\pi)^3 \rho} \tilde{v}_{\text{LS}}^2(q) \int_0^\infty \frac{d\omega}{\pi} \text{Im} \chi_0(q; \omega) \chi_0^{(\perp)}(q, \omega). \quad (2.47)$$

This is so far standard second-order perturbation theory. The expression (2.47) is now easily generalized to the sum of all ring-diagrams by replacing one of the bare interactions  $\tilde{v}_{\text{LS}}(q)$  by  $\tilde{V}_{\text{p-h}}^{(\text{LS})}(q)$ , one by  $\tilde{W}^{(\text{LS})}(q)$  defined in Eq. (2.29), and performing the usual coupling constant integration [73]. We hasten to point out that using the expression (2.22) leads to the same answer,

$$\begin{aligned} \frac{\Delta E_{\text{ring}}}{N} &= -\frac{1}{4} \sum_{\alpha \in \{\text{c}, \text{T}\}} \int \frac{d^3 q}{(2\pi)^3 \rho} \int_0^\infty \frac{d\omega}{\pi} \int_0^1 d\lambda \text{Im} \frac{[\tilde{V}_{\text{p-h}}^{(\text{LS})}(q)]^2 \chi_0(q; \omega) \chi_0^{(\perp)}(q, \omega)}{1 - \lambda \tilde{V}_{\text{p-h}}^{(\alpha)}(q, \omega) \chi_0(q; \omega)} \\ &= \frac{1}{4} \sum_{\alpha \in \{\text{c}, \text{T}\}} \int \frac{d^3 q}{(2\pi)^3 \rho} \int_0^\infty \frac{d\omega}{\pi} \frac{[\tilde{V}_{\text{p-h}}^{(\text{LS})}(q)]^2 \chi_0^{(\perp)}(q, \omega)}{\tilde{V}_{\text{p-h}}^{(\alpha)}(q, \omega)} \ln [1 - \tilde{V}_{\text{p-h}}^{(\alpha)}(q, \omega) \chi_0(q; \omega)]. \end{aligned} \quad (2.48)$$

### D. Inclusion of exchange diagrams

Corrections to the RPA are often discussed in terms of two different effects: One is the modification of the single-

particle Green's functions by self-energy corrections, and the second is the inclusion of exchange terms of the particle-hole interaction. Figure 1 shows the lowest order terms in the

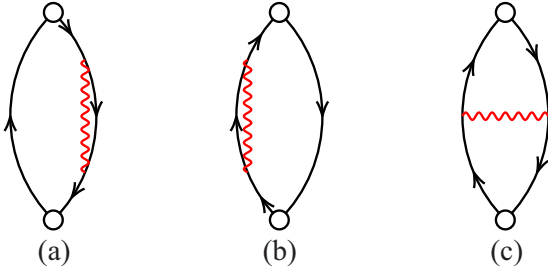


FIG. 1. Goldstone diagrams representing the first-order corrections to the RPA using the usual conventions of Goldstone perturbation theory. Diagram (a) is a self-energy correction to a hole propagator, diagram (b) a correction to the particle propagator, whereas diagram (c) is the first correction coming from including exchanges in the RPA. The wiggly red line represents an interaction.

conventions of Goldstone perturbation theory. Figure 1(a) is the contribution of the Hartree-Fock exchange term to the hole propagator, Fig. 1(b) to the particle propagator, and Fig. 1(c) shows an RPA exchange diagram.

Corrections to the single-particle Green's function are, of course, much more easily treated than exchange terms because one is dealing with a one-body quantity. The treatment of exchanges is more complicated; see for example Ref. [74]. Therefore, the two effects are normally treated separately, often just leaving one of them out.

It is, of course, well known that *both* contributions must be retained to satisfy the energy weighted sum rule. The diagrammatic analysis of Jastrow-Feenberg wave functions comes to a similar picture: Fig. 2 shows three diagrams of the

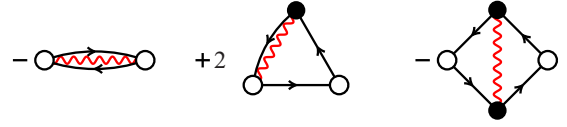


FIG. 2. First-order exchange diagrams in the FHNC diagrammatic language. Oriented solid lines represent FHNC exchange lines, the wiggly red line represents either a correlation or effective interaction line.

Jastrow-Feenberg variational theory for Fermions that have the same momentum flux as the Goldstone diagrams of Fig. 1. In fact, the analysis of the diagrams of the Jastrow-Feenberg variational theory in terms of Goldstone diagrams [28,75] leads to the conclusion that the diagrams shown in Fig. 2 are indeed approximations to the Goldstone diagrams shown in Fig. 1.

From the point of view of Jastrow-Feenberg theory there is ample evidence that there is a strong cancellation between the three diagrams shown in Fig. 2. Among others, keeping these terms together is a necessary condition for obtaining meaningful solutions of the variational problem (1.6) [69,76].

Concluding that these diagrams should either all be kept or all be left out, we have dealt with exchange effects as described in Refs. [6,28]: The first-order exchange diagram depends rigorously on both hole momenta  $\mathbf{h}$ ,  $\mathbf{h}'$  and the momentum transfer  $\mathbf{q}$ :

$$W_{\text{ex}}(\mathbf{h}, \mathbf{h}'; \mathbf{q}) = \Omega(\mathbf{h} + \mathbf{q}, \mathbf{h}' - \mathbf{q})W|\mathbf{h}', \mathbf{h}\rangle. \quad (2.49)$$

We have approximated this nonlocal quantity by a function of momentum transfer by calculating the Fermi-sea average

$$\tilde{V}_{\text{ex}}(q) \equiv \langle W_{\text{ex}} \rangle(q) = \frac{\sum_{\mathbf{h}\mathbf{h}'} n(\mathbf{h})n(\mathbf{h}')\bar{n}(|\mathbf{h} + \mathbf{q}|)\bar{n}(|\mathbf{h}' - \mathbf{q}|)\Omega(\mathbf{h} + \mathbf{q}, \mathbf{h}' - \mathbf{q})W|\mathbf{h}', \mathbf{h}\rangle}{[\sum_{\mathbf{h}} \bar{n}(|\mathbf{h} + \mathbf{q}|)n(\mathbf{h})]^2}. \quad (2.50)$$

In fact, the averaging procedure (2.50) is used at several places to establish the connection between the Jastrow-Feenberg variational theory and the parquet-diagram summations. More details on the procedure and how the Euler equations are modified by the inclusion of exchange diagrams are discussed in Refs. [6,28].

### III. RESULTS AND SUMMARY

#### A. Interactions

We have mostly employed for our calculations the Argonne [4] interaction because it is formulated in terms of the operator expansion (1.1). The Reid interaction [1] has been formulated only in a  $v_6$  form [3]. To generate a  $v_8$  version of the Reid interaction we have followed the procedure of Ref. [4]. For the sake of discussion, let  $v_\alpha^{(n)}(r_{ij})$  be the coefficient of the operator  $\hat{O}_\alpha(i, j)$  in a  $v_n$  representation of the interaction. Reference [4] generates a  $v_6$  approximation from a  $v_8$  form by

$$V_{\text{cc}}^{(6)}(r) = V_{\text{cc}}^{(8)}(r) - \frac{0.9}{16}[V_{\text{c,LS}}(r) - 3V_{\text{\tau,LS}}(r)], \quad (3.1a)$$

$$V_{\text{c}\tau}^{(6)}(r) = V_{\text{c}\tau}^{(8)}(r) + \frac{0.9}{16}[V_{\text{c,LS}}(r) - 3V_{\text{\tau,LS}}(r)], \quad (3.1b)$$

$$V_{\text{\sigma c}}^{(6)}(r) = V_{\text{\sigma c}}^{(8)}(r) - \frac{0.3}{16}[V_{\text{c,LS}}(r) - 3V_{\text{\tau,LS}}(r)], \quad (3.1c)$$

$$V_{\text{\sigma}\tau}^{(6)}(r) = V_{\text{\sigma}\tau}^{(8)}(r) + \frac{0.3}{16}[V_{\text{c,LS}}(r) - 3V_{\text{\tau,LS}}(r)]. \quad (3.1d)$$

We have used this procedure to generate a  $v_8$  representation of the Reid interaction as follows: The spin-orbit potential components  $V_{\text{c,LS}}(r)$  and  $V_{\text{\tau,LS}}(r)$  were constructed from the isospin = 0 and isospin = 1 components of the Reid interaction; cf. Eqs. (20) and (30) of Ref. [1]. The four components  $V_\alpha^{(6)}(r)$ ,  $\alpha \in \{\text{cc}, (\text{c}\tau), (\sigma\text{c}), (\sigma\tau)\}$  were taken from Eqs. (A3)–(A8) of Ref. [3]. Then we used Eqs. (3.1a)–(3.1d) to construct a  $v_8$  representation of the Reid interaction.

Another interaction that is given in the operator basis is the one of Wiringa, Smith, and Ainsworth [5]. This interaction has been used by Smith and Jackson [37] in a  $v_6$  calculation of a fictitious system of interacting bosons. These authors argue that the spin-orbit interaction can indeed have a visible effect



in nuclear matter. We have not been able to verify this in neutron matter and leave the issue to further study.

### B. Long-wavelength limit

The most important input for linear response theory and, hence, for the calculation of the dynamic structure function, is the particle-hole interaction. The hydrodynamic speed of sound

$$mc^2 = \frac{d}{d\rho} \rho^2 \frac{d}{d\rho} \frac{E}{N} \quad (3.2)$$

is related to the long-wavelength limit of the particle-hole interaction. In a Fermi fluid, we also have Pauli repulsion, reflected in the relation

$$mc^2 = mc_F^{*2} + \tilde{V}_{p-h}(0+) \equiv mc_F^{*2}(1 + F_0^S), \quad (3.3)$$

where  $c_F^* = \sqrt{\frac{\hbar^2 k_F^2}{3mm^*}}$  is the speed of sound of the non-interacting Fermi gas with the effective mass  $m^*$ , and  $F_0^S$  is Landau's Fermi liquid parameter. In neutron matter we can safely set  $m^* = m$  [77]. We note in passing that the local approximation (2.50) gives the correct contribution to  $mc^2$  as defined in Eq. (3.3) from the leading-order exchange diagrams [76].

The relationships (3.2) and (3.3) give identical predictions only in an exact theory [76,78]; good agreement is typically reached only at very low densities. Even in the much simpler system  ${}^4\text{He}$ , where four- and five-body elementary diagrams and three-body correlations are routinely included, the two expressions (3.2) and (3.3) can differ by up to a factor of 2 [79].

The situation is even more complicated in Fermi systems, again due to the multitude of exchange diagrams, of which we kept only the simplest. Hence, one can expect good agreement only at very low densities [28], but not at the densities considered here. To make valid predictions on the density-density response function we have followed here the procedure of Ref. [79] and added a phenomenological component to the theory: We have scaled, for  $q \leq 2k_F$  the exchange correction  $\tilde{V}_{ex}(q)$  such that the two expressions (3.2) and (3.3) agree. The procedure has no visible effect on the equation of state. One can think of a similar procedure for  $\tilde{V}_{p-h}^{(L)}(0+)$ , by comparing the microscopically calculated Landau parameter with a magnetic susceptibility obtained by calculating the equation of state for partially spin-polarized systems.

### C. Effective spin-orbit interaction

One of the main focuses of interest is, of course, the consequences of many-body correlations on effective interactions. We have introduced above the ‘‘particle-hole interaction’’  $\hat{V}_{p-h}(\mathbf{q})$  [cf. Eq. (2.40)], the effective interactions  $\hat{W}(\mathbf{q}; \omega)$ , and the induced interaction  $\hat{w}_I(\mathbf{q}; \omega)$ , Eq. (2.6), as well as their energy-independent counterparts.

The tensor force breaks, in the spin-triplet case  $S = 1$ , the degeneracy of the correlations in the  $M_S = 1$  and the  $M_S = 0$  channels, described by  $\Gamma^{(t+)}(r)$  and  $\Gamma^{(t-)}(r)$ . This would lead to *two different* spin-orbit particle-hole interactions for  $M_S = 0$  and  $M_S = 1$ ; see Eq. (2.40). We have taken in Eq. (2.40)

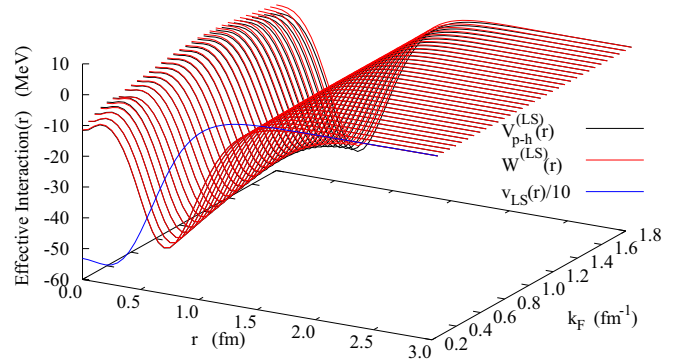


FIG. 3. The figure shows the particle-hole interaction  $V_{p-h}^{(LS)}(r)$  (black lines), the effective interaction  $W^{(LS)}(r)$  (red lines), and, for comparison, the bare spin-orbit interaction (blue line). The bare interaction has been scaled by a factor 0.1 to fit into the plot.

generally the  $M_S = 1$  projection for two reasons: For most of the calculations to follow, the influence of the spin-orbit interaction is small. This is because the corrections to the effective interactions are quadratic in the spin-orbit potential; see Eqs. (2.17a) and (2.17b). We found that using the  $M_S = 0$  projection of the correlation leads to an even smaller correction from the spin-orbit terms. The second reason is that the likely most prominent influence of the spin-orbit effective interaction is on  ${}^3P_2$  pairing in high-density neutron matter. In that case, the  $M_S = 1$  channel is the appropriate one. We also stress that, in this case, neither of the local approximations discussed in Sec. II A 4 is necessary; in fact it is more appropriate to calculate the effective interaction for  $\hbar\omega = 0$  [29].

Figure 3 shows the particle-hole interaction  $V_{p-h}^{(LS)}(r)$ , the static effective interaction  $W^{(LS)}(r)$ , and the bare spin-orbit potential [4]. Evidently, the full effective interaction and the particle-hole interaction are almost indistinguishable; their difference is certainly less than the accuracy of the parquet//1 approximation used here. That says that ‘‘induced interaction’’ effects to the spin-orbit component of the effective interaction are negligible. This of course does not imply that the induced interaction is negligible for the other components of the interaction; see Figs. 10 and 11 of Ref. [6].

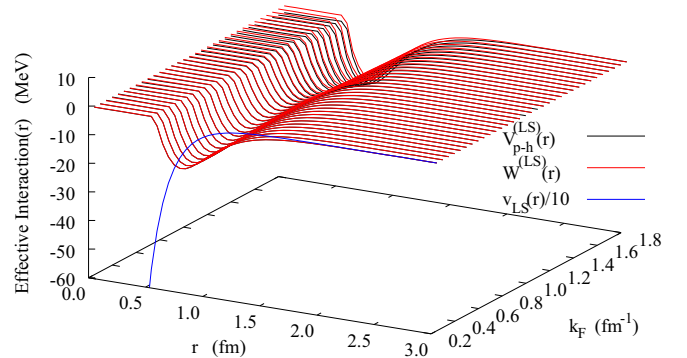


FIG. 4. Same as Fig. 3 for our  $v_8$  formulation of the Reid interaction.

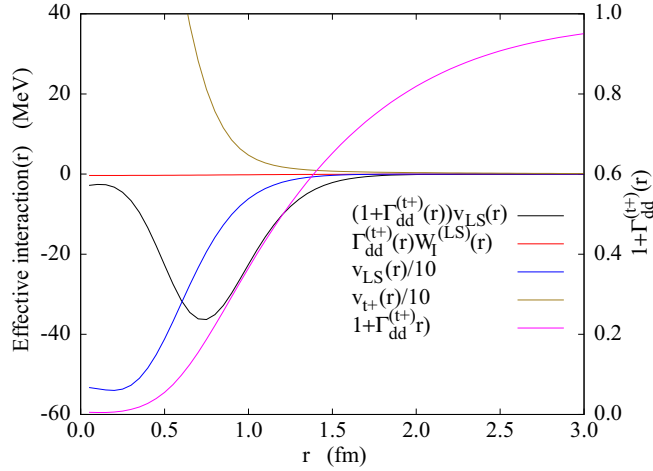


FIG. 5. The figure shows, for  $k_F = 1.0 \text{ fm}^{-1}$ , the individual contributions to the effective spin-orbit interaction (left scale). We also show the direct correlation function  $1 + \Gamma_{dd}^{(t+)}(r)$  in the  $t+$  projector channel (magenta line, right scale) and the bare interactions  $v_{LS}(r)$  and  $v_{t+}(r)$  of the Argonne potential. These were scaled by a factor of 0.1 to fit into the plot.

The most prominent effect that modifies the bare interaction in the spin-orbit channel is the screening of its short-ranged behavior by the correlations caused by the surrounding particles. This screening is manifested in the factor  $1 + \Gamma_{dd}^{(t+)}(r)$  in Eq. (2.40). Thus, our result is that the effective interaction has very little resemblance to the bare interaction, but that a relatively simple treatment of correlations is adequate to deal with many-body effects.

The situation is very similar for the  $v_8$  representation of the Reid potential; see Fig. 4. The spin-orbit component of the Reid interaction is singular as  $r \rightarrow 0$ , thus it appears to be much stronger than the bare spin-orbit interaction from the Argonne potential. However, the short-ranged screening is also stronger, resulting in an effective interaction that is similar to the one derived from the Argonne potential.

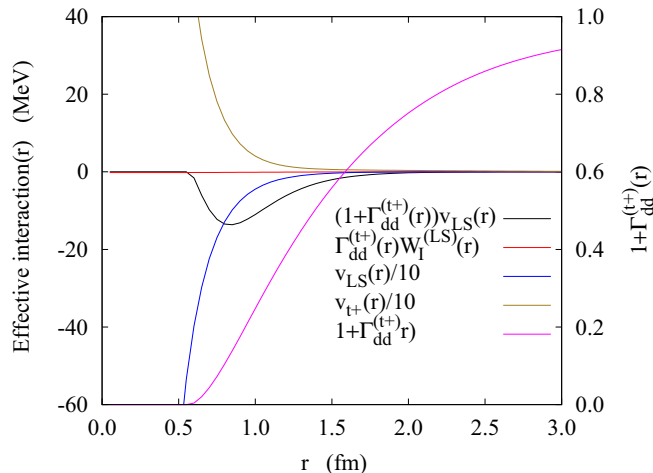


FIG. 6. Same as Fig. 5 for the Reid interaction.

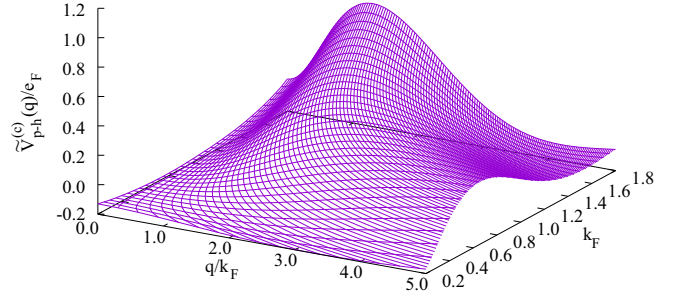


FIG. 7. The figure shows the central component  $\tilde{V}_{p-h}^{(c)}(q)$  of the particle-hole interaction in units of the Fermi energy of the noninteracting system.

More details on the different contributions to the effective interactions are shown in Figs. 5 and 6. The figures show, at the representative density  $k_F = 1.0 \text{ fm}^{-1}$ , the decomposition (2.40) of the particle-hole interaction into the short-ranged screening effect  $v_{LS}(r)[1 + \Gamma_{dd}^{(t+)}(r)]$  and the induced interaction  $\Gamma_{dd}^{(t+)}(r)w_1^{(LS)}(r)$ . We also show, for comparison, the bare interactions  $v_{LS}(r)$  and  $v_{t+}(r)$ . The comparison offers an explanation for why the spin-orbit potential is strongly suppressed by many-body correlations. The pair correlation  $1 + \Gamma_{dd}^{(t+)}(r)$  is predominantly determined by  $v_{t+}(r)$ , which is strongly repulsive. Hence, the correlation function tends to suppress the interaction.

Figure 6 shows the same data for the  $v_8$  version of the Reid potential. On the other hand, the  $t+$  component of the Reid interaction is slightly more repulsive than that of the Argonne potential, causing a somewhat stronger short-ranged screening. As a result, the spin-orbit component of the effective interactions is even smaller than that of the Argonne potential.

#### D. Corrections to the particle-hole interactions in the central and transverse channels

The essential input to the calculation of the density-density response function is the particle-hole interaction. The spin-orbit potential contributes a relatively small energy-dependent correction. Figures 7 and 8 show  $\tilde{V}_{p-h}^{(c)}(q)$  and  $\tilde{V}_{p-h}^{(T)}(q)$ ; the results differ visibly from those obtained in Ref. [6] by the

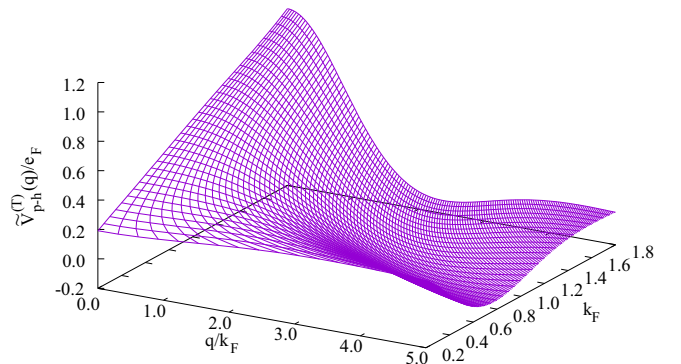


FIG. 8. Same as Fig. 7 for the transverse component  $\tilde{V}_{p-h}^{(T)}(q)$  of the particle-hole interaction.

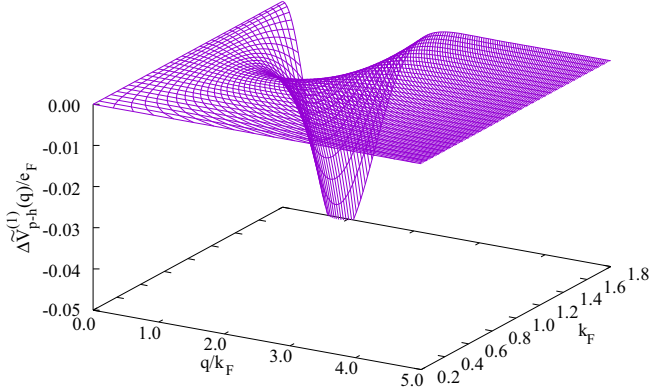


FIG. 9. The figure shows the correction spelled out in Eq. (2.17a) to the central part of the particle-hole interaction, Fig. 7, taken at the average energy  $\hbar\omega_F(q) = t(q)/S_F(q)$ .

inclusion of nonparquet “twisted chain” contributions and the modification of the exchange interaction discussed in Sec. III B.

Figure 9 finally shows the correction (2.17a) due to spin-orbit interaction; note that the correction to the transverse channel is half of that [see Eq. (2.17b)]. Evidently the correction is very small. This is due to two effects, namely that the spin-orbit correction is of second order and that the spin-orbit force gets effectively screened by many-body correlations of the surrounding medium; see Fig. 5.

We conclude this section by remarking that the correction (2.48) has turned out to be less than 0.1 MeV, which is of the order of a percent of the total energy. It is therefore not shown here.

### E. Dynamic structure function

In what follows we focus on results obtained for the Argonne interaction; those for the Reid potential are quite similar and nothing can be learned from a comparison.

The dynamic structure function of nuclear and neutron matter has been the subject of intense studies literally for decades; see among others Ref. [53] for very early work.

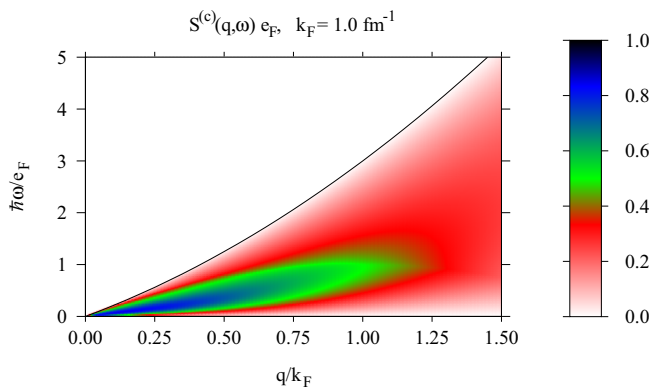


FIG. 10. The figure shows a color map of the density channel  $S^{(c)}(q, \omega)$  of the dynamic structure function at  $k_F = 1.0 \text{ fm}^{-1}$ . The solid line is the upper boundary of the particle-hole continuum.

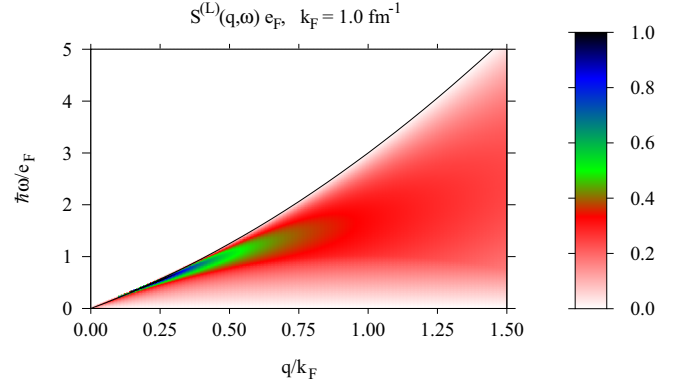


FIG. 11. Same as Fig. 10 for the longitudinal channel  $S^{(L)}(q, \omega)$  of the dynamic structure function.

These calculations were typically at the RPA level; interactions were taken either semi-phenomenologically using simplified nucleon-nucleon interactions [53,74,80], effective Skyrme interactions [44–46,49–52], or pseudopotentials [54]. Closest to our formulation and philosophy is the pseudopotential method. In fact, the phenomenological considerations that went into the construction of pseudopotentials for the helium liquids [41,81] are faithfully reproduced and thereby justified by microscopic calculations [69,82]. Developing pseudopotentials is of course much more complicated in neutron and nuclear matter due to the absence of extensive experimental data; phenomenological theories therefore suffer from more ambiguities. There are only a few low-order calculations that attempt to include correlation effects in the dynamic response [83–85].

In our microscopic calculations, the response of the system to the external fields (2.23) is naturally formulated in terms of the operators  $\mathbb{1}$ ,  $\hat{L}$ , and  $\hat{T}$ ; see Eq. (2.24). The tensor force breaks the degeneracy in  $\hat{L}$  and  $\hat{T}$ .

A first overview of our results is given in Figs. 10–12. We show there results for  $k_F = 1.0 \text{ fm}^{-1}$ ; the results for different densities are rather similar. The most evident difference between the distinct channels is that the strength of  $S^{(c)}(q, \omega)$  is mostly in the middle of the particle-hole continuum whereas

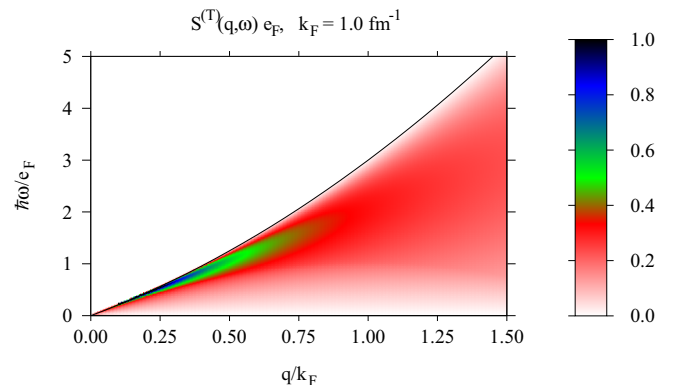


FIG. 12. Same as Fig. 10 for the transverse channel  $S^{(T)}(q, \omega)$  of the dynamic structure function.

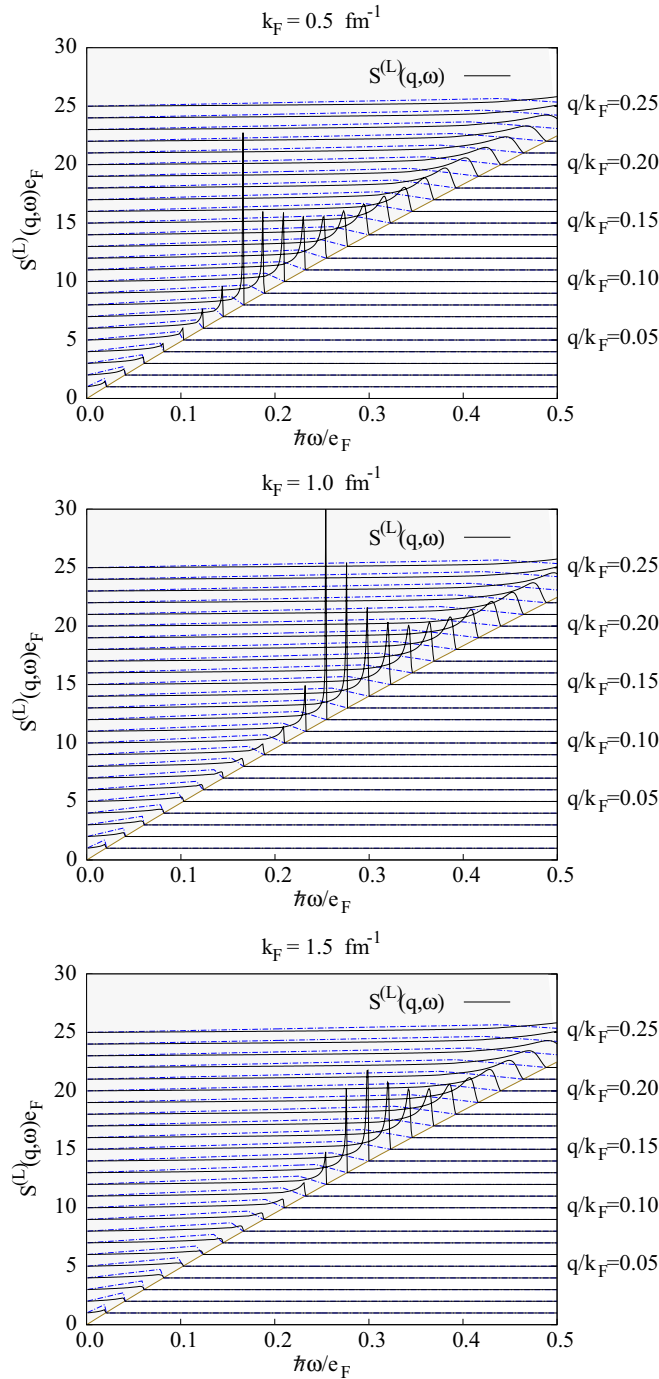


FIG. 13. The figures show details of  $S^{(L)}(q, \omega)$  for three densities as indicated in the plots for momentum transfers  $q/k_F = 0.01, \dots, 0.25$ . The individual results are stacked as indicated on the right side of the plots. The dashed blue lines show, for comparison, the dynamic structure function of the noninteracting system, and the gray-shaded area shows the particle-hole continuum.

$S^{(L)}(q, \omega)$  and  $S^{(T)}(q, \omega)$  show, at long wavelengths, significant strength just below the boundary of the particle-hole continuum. Our results are in that aspect similar to those obtained with Skyrme interactions [45,46] and at low cluster

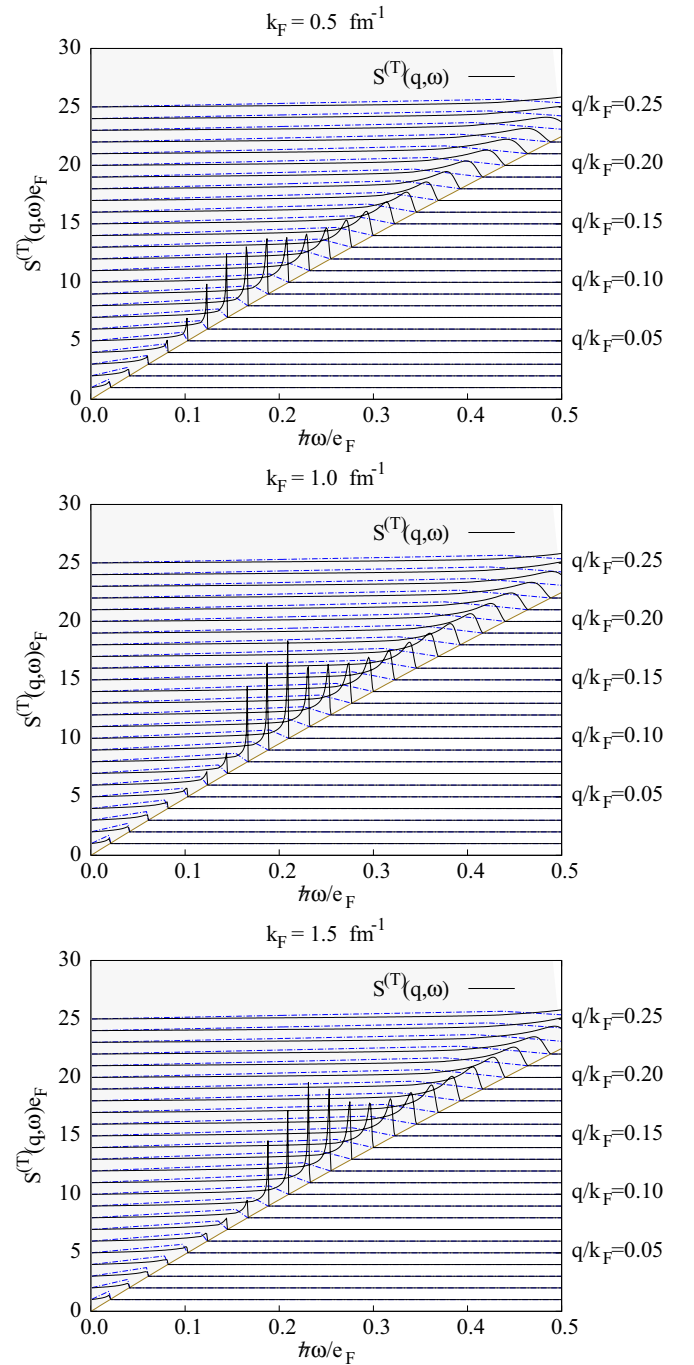


FIG. 14. Same as Fig. 13 for  $S^{(T)}(q, \omega)$ .

orders [85], which occasionally find that mode outside the continuum.

Let us therefore have a closer look at the long-wavelength properties at different densities. Details are shown in Figs. 13 and 14. The peaks in both  $S^{(L)}(q, \omega)$  and  $S^{(T)}(q, \omega)$  are clearly seen; the figures also substantiate the remark made above that the results are rather similar at different densities.

The peak in  $S^{(L)}(q, \omega)$  and  $S^{(T)}(q, \omega)$  is caused by a node of the real part of the denominators in Eqs. (2.24), i.e., by the

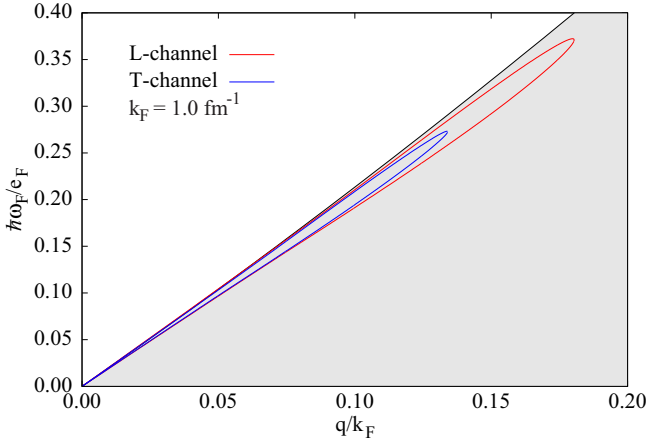


FIG. 15. The figure shows the location of the solution of Eq. (3.4) for  $\alpha = L$  and  $\alpha = T$ . The gray shaded area is the particle-hole continuum.

solution of

$$\text{Re} \left[ 1 - \tilde{V}_{\text{p-h}}^{(\alpha)}(q, \omega_{\text{zs}}(q)) \chi_0(q, \omega_{\text{zs}}(q)) \right] = 0, \quad (3.4)$$

with  $\omega_{\text{zs}}(q)$  being the zero-sound mode.

In our case, the solutions of Eq. (3.4) are inside the continuum; that means the imaginary part is nonzero but evidently very small. Figure 15 shows, for  $k_F = 1.0 \text{ fm}^{-1}$ , the location of the “zero sound pole” for longitudinal and transverse excitations.

A closer look at the strength distribution in  $S^{(\alpha)}(q, \omega)$  is provided in Fig. 16. Similar to what we have seen above, the strength in the central channel is broadly distributed within the particle-hole continuum whereas the strength of the two spin modes is shifted towards the upper boundary. This holds quite well up to  $q \approx 0.5 k_F$  although the node of Eq. (3.4) disappears at  $q < 0.2 k_F$ . With increasing momentum transfer the structure functions become closer to the noninteracting limit. The same holds at other densities.

### F. Summary

In this work we developed the parquet-diagram summation method for the  $v_8$  model of the nucleon-nucleon interaction. Our results have been threefold:

We first derived closed-form expressions for the effective interaction. These are nonlocal and are *not* of the  $v_8$  form but contain three more operators,  $\hat{Q}_7$ ,  $\hat{Q}_9$ , and  $\tilde{L}S'$  [Eqs. (2.14b) and (2.14c)]. Additionally, these interactions are energy dependent. As long as one just needs these interactions, for example, for the examination of pairing phenomena, there is no need for further approximations. Only for the purpose of parquet-diagram summations were local approximations to these effective interactions introduced in Sec. II A 4.

Next we examined, in Sec. III C, the effect of correlations on the spin-orbit interaction. We have demonstrated in Figs. 3–6 that many-body correlations have a rather drastic screening effect. The induced interaction,

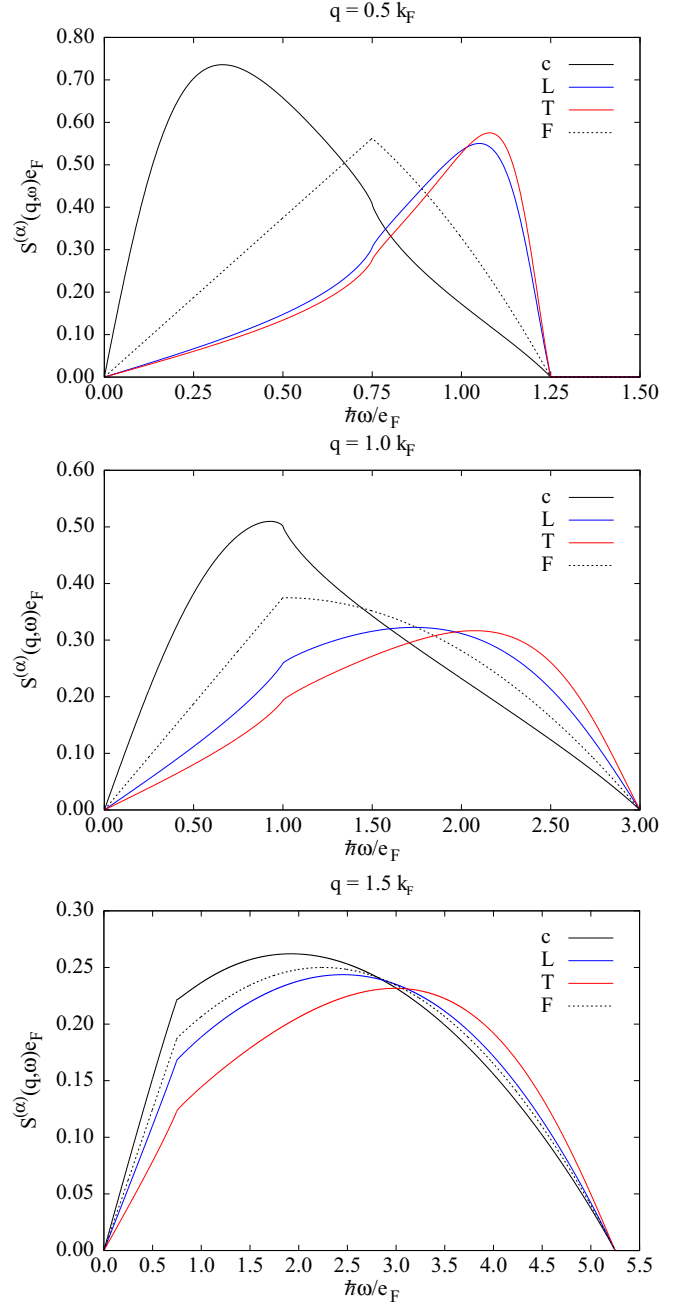


FIG. 16. The figure shows, for  $k_F = 1.0 \text{ fm}^{-1}$ , the c (black line), L (blue line), and T (red line) components of the dynamic structure function at  $q = 0.5, 1.0, 1.5 k_F$ . The black dashed line is the dynamic structure function of the non-interacting Fermi system.

which plays a visible role in  $S$ -wave pairing effects, is almost negligible in the spin-orbit channel whereas it is quite visible in the central, longitudinal, and transverse channels [6,7].

Finally, we have joined the long sequence of works dealing with the (spin-)density response functions of neutron matter. Our work is distinguished from most of the previous work in the sense that it is manifestly microscopic whereas Skyrme interactions or pseudopotentials require significant

phenomenological input which is sometimes hard to justify in a fictitious system like neutron matter. Closest to our work are early calculations by Kwong [83] and calculations at the three-body cluster level [85].

We found that, apart from the direct calculation of spin-orbit effective interaction, the effect of the spin-orbit potential is rather small. In particular, we found that the energy correction (2.48) is negligibly small.

## APPENDIX A: DETAILS OF THE CHAINING OPERATIONS

We present in this Appendix details of the calculation of the effective potential  $\hat{W}(\mathbf{q})$  containing a spin-orbit interaction. Let us begin with the case in which the particle-hole interaction consists of a spin-orbit term alone; we will then combine our results with the other channels. The particle-hole spin-orbit interaction in momentum space is then simply

$$\hat{V}_{\text{p-h}}^{(\text{LS})}(\mathbf{q}) = \tilde{V}_{\text{p-h}}^{(\text{LS})}(q) \widetilde{\mathbf{L}} \cdot \mathbf{S}. \quad (\text{A1})$$

### 1. Chains of pure spin-orbit operators

We begin with the second-order convolution product,

$$\begin{aligned} \hat{W}_{\text{LS}}^{(2)}(\mathbf{q}, \mathbf{h}, \mathbf{h}', \boldsymbol{\sigma}, \boldsymbol{\sigma}'; \omega) &= [\hat{V}_{\text{p-h}}^{(\text{LS})}(\mathbf{q}) * \chi_0 * \hat{V}_{\text{p-h}}^{(\text{LS})}(\mathbf{q})] \\ &= \frac{1}{N} [\tilde{V}_{\text{p-h}}^{(\text{LS})}(q)]^2 \text{Tr}_{\boldsymbol{\sigma}''} \sum_{\mathbf{h}''} \left[ i\hat{\mathbf{q}} \times (\mathbf{h}_{\text{F}} - \mathbf{h}_{\text{F}}'') \cdot \frac{1}{2}(\boldsymbol{\sigma} + \boldsymbol{\sigma}'') \right] \chi_0(\mathbf{q}, \mathbf{h}''; \omega) \left[ i\hat{\mathbf{q}} \times (\mathbf{h}_{\text{F}}'' - \mathbf{h}_{\text{F}}') \cdot \frac{1}{2}(\boldsymbol{\sigma}'' + \boldsymbol{\sigma}') \right]. \end{aligned} \quad (\text{A2})$$

All terms with a single  $\boldsymbol{\sigma}''$  operator vanish because  $\text{Tr}_{\boldsymbol{\sigma}''} \boldsymbol{\sigma}'' = 0$ . Also, all first-order terms in  $(\hat{\mathbf{q}} \times \mathbf{h}_{\text{F}}'')$  vanish because of azimuthal symmetry,  $\sum_{\mathbf{h}''} (\hat{\mathbf{q}} \times \mathbf{h}_{\text{F}}'') \chi_0(q, \mathbf{h}''; \omega) = 0$ . Thus, we are left with

$$\begin{aligned} \hat{W}_{\text{LS}}^{(2)}(\mathbf{q}, \mathbf{h}, \mathbf{h}', \boldsymbol{\sigma}, \boldsymbol{\sigma}'; \omega) &= \frac{[\tilde{V}_{\text{p-h}}^{(\text{LS})}(q)]^2}{4N} \sum_{\mathbf{h}''} \chi_0(\mathbf{q}, \mathbf{h}''; \omega) \text{Tr}_{\boldsymbol{\sigma}''} \{ [(\hat{\mathbf{q}} \times \mathbf{h}_{\text{F}}) \cdot \boldsymbol{\sigma}] [(\hat{\mathbf{q}} \times \mathbf{h}_{\text{F}}') \cdot \boldsymbol{\sigma}'] + [(\hat{\mathbf{q}} \times \mathbf{h}_{\text{F}}') \cdot \boldsymbol{\sigma}] [(\hat{\mathbf{q}} \times \mathbf{h}_{\text{F}}) \cdot \boldsymbol{\sigma}'] \\ &\quad + [(\hat{\mathbf{q}} \times \mathbf{h}_{\text{F}}) \cdot \boldsymbol{\sigma}''] [(\hat{\mathbf{q}} \times \mathbf{h}_{\text{F}}') \cdot \boldsymbol{\sigma}''] + [(\hat{\mathbf{q}} \times \mathbf{h}_{\text{F}}') \cdot \boldsymbol{\sigma}''] [(\hat{\mathbf{q}} \times \mathbf{h}_{\text{F}}) \cdot \boldsymbol{\sigma}''] \}. \end{aligned} \quad (\text{A3})$$

Carrying out the  $\boldsymbol{\sigma}''$  summation gives the final result,

$$\begin{aligned} \hat{W}_{\text{LS}}^{(2)}(\mathbf{q}, \mathbf{h}, \mathbf{h}', \boldsymbol{\sigma}, \boldsymbol{\sigma}'; \omega) &= \frac{1}{4} [\tilde{V}_{\text{p-h}}^{(\text{LS})}(q)]^2 [\chi_0^{(\perp)}(q; \omega) \left[ \mathbb{1} + \frac{1}{2} \hat{T} \right] + \chi_0(q; \omega) \left[ \hat{Q}_7 + \frac{1}{2} \hat{Q}_9 \right]] \\ &\equiv \sum_{\alpha, \text{odd}} \tilde{W}_{\text{LS}}^{(2, \alpha)}(q; \omega) \hat{Q}_\alpha \end{aligned} \quad (\text{A4})$$

where we have introduced the two additional operators

$$\hat{Q}_7 \equiv [(\hat{\mathbf{q}} \times \mathbf{h}_{\text{F}}) \cdot \boldsymbol{\sigma}] [(\hat{\mathbf{q}} \times \mathbf{h}_{\text{F}}') \cdot \boldsymbol{\sigma}'], \quad (\text{A5a})$$

$$\hat{Q}_9 \equiv 2(\hat{\mathbf{q}} \times \mathbf{h}_{\text{F}}) \cdot (\hat{\mathbf{q}} \times \mathbf{h}_{\text{F}}'); \quad (\text{A5b})$$

see Eqs. (2.14b). From the orthogonality relations (2.15) we can conclude that the sum of all chain diagrams containing an even number of spin-orbit interaction operators  $\hat{V}_{\text{p-h}}^{(\text{LS})}(\mathbf{q})$  and no other interaction component can be written as

$$\hat{W}_{\text{LS}}^{(\text{even})}(\mathbf{q}, \mathbf{h}, \mathbf{h}', \boldsymbol{\sigma}, \boldsymbol{\sigma}'; \omega) = \sum_{\alpha} \tilde{W}_{\text{LS}}^{(\text{even}, \alpha)}(q; \omega) \hat{Q}_\alpha \quad (\text{A6})$$

with

$$\tilde{W}_{\text{LS}}^{(\text{even}, c)}(q; \omega) = \frac{1}{4} \frac{[\tilde{V}_{\text{p-h}}^{(\text{LS})}(q)]^2 \chi_0^{(\perp)}(q; \omega)}{1 - \frac{1}{4} \chi_0(q; \omega) \chi_0^{(\perp)}(q; \omega) [\tilde{V}_{\text{p-h}}^{(\text{LS})}(q)]^2}, \quad (\text{A7a})$$

$$\tilde{W}_{\text{LS}}^{(\text{even}, T)}(q; \omega) = \frac{1}{8} \frac{[\tilde{V}_{\text{p-h}}^{(\text{LS})}(q)]^2 \chi_0^{(\perp)}(q; \omega)}{1 - \frac{1}{8} \chi_0(q; \omega) \chi_0^{(\perp)}(q; \omega) [\tilde{V}_{\text{p-h}}^{(\text{LS})}(q)]^2}, \quad (\text{A7b})$$

$$\tilde{W}_{\text{LS}}^{(\text{even}, 7)}(q; \omega) = \frac{1}{4} \frac{[\tilde{V}_{\text{p-h}}^{(\text{LS})}(q)]^2 \chi_0(q; \omega)}{1 - \frac{1}{4} \chi_0(q; \omega) \chi_0^{(\perp)}(q; \omega) [\tilde{V}_{\text{p-h}}^{(\text{LS})}(q)]^2}, \quad (\text{A7c})$$

$$\tilde{W}_{\text{LS}}^{(\text{even},9)}(q; \omega) = \frac{1}{8} \frac{[\tilde{V}_{\text{p-h}}^{(\text{LS})}(q)]^2 \chi_0(q; \omega)}{1 - \frac{1}{8} \chi_0(q; \omega) \chi_0^{(\perp)}(q; \omega) [\tilde{V}_{\text{p-h}}^{(\text{LS})}(q)]^2}. \quad (\text{A7d})$$

There is no contribution to the longitudinal channel  $\tilde{W}_{\text{LS}}^{(\text{even},L)}(q; \omega)$ .

To obtain the odd-order chains, one needs to introduce one more new operator,

$$\tilde{\text{LS}}' \equiv \frac{i}{2} [(\hat{\mathbf{q}} \times \mathbf{h}_{\text{F}}) \cdot \boldsymbol{\sigma} - (\hat{\mathbf{q}} \times \mathbf{h}'_{\text{F}}) \cdot \boldsymbol{\sigma}']. \quad (\text{A8})$$

For the further manipulations we need the following convolution properties:

$$[\mathbb{1} * \chi_0 * \tilde{\text{L}} \cdot \tilde{\text{S}}] = -\frac{i}{2} \chi_0(q; \omega) (\hat{\mathbf{q}} \times \mathbf{h}'_{\text{F}}) \cdot \boldsymbol{\sigma}', \quad (\text{A9a})$$

$$[\hat{T} * \chi_0 * \tilde{\text{L}} \cdot \tilde{\text{S}}] = -\frac{i}{2} \chi_0(q; \omega) (\hat{\mathbf{q}} \times \mathbf{h}'_{\text{F}}) \cdot \boldsymbol{\sigma}, \quad (\text{A9b})$$

$$[\tilde{\text{LS}}' * \chi_0 * \tilde{\text{L}} \cdot \tilde{\text{S}}] = \frac{1}{4} [\chi_0(q; \omega) \hat{Q}_7 + \chi_0^{(\perp)}(q; \omega) \mathbb{1}], \quad (\text{A9c})$$

$$[\hat{Q}_7 * \chi_0 * \tilde{\text{L}} \cdot \tilde{\text{S}}] = \frac{i}{2} \chi_0^{(\perp)}(q; \omega) (\hat{\mathbf{q}} \times \mathbf{h}_{\text{F}}) \cdot \boldsymbol{\sigma}, \quad (\text{A9d})$$

$$[\hat{Q}_9 * \chi_0 * \tilde{\text{L}} \cdot \tilde{\text{S}}] = i \chi_0^{(\perp)}(q; \omega) (\hat{\mathbf{q}} \times \mathbf{h}_{\text{F}}) \cdot \boldsymbol{\sigma}', \quad (\text{A9e})$$

$$[\mathbb{1} * \chi_0 * \tilde{\text{LS}}'] = -\frac{i}{2} \chi_0(q; \omega) (\hat{\mathbf{q}} \times \mathbf{h}'_{\text{F}}) \cdot \boldsymbol{\sigma}', \quad (\text{A9f})$$

$$[\hat{T} * \chi_0 * \tilde{\text{LS}}'] = 0. \quad (\text{A9g})$$

The reversed order of operators, i.e.,  $[\hat{O}_i * \chi_0 * \hat{O}_j] \leftrightarrow [\hat{O}_j * \chi_0 * \hat{O}_i]$ , is obtained by exchanging  $\mathbf{h}_{\text{F}} \leftrightarrow \mathbf{h}'_{\text{F}}$ ,  $\boldsymbol{\sigma} \leftrightarrow \boldsymbol{\sigma}'$ , and  $i \leftrightarrow -i$ . From that, we obtain that the sum of all odd-power pure  $\hat{V}_{\text{p-h}}^{(\text{LS})}(\mathbf{q})$  chains is a linear combination of the operators  $\tilde{\text{L}} \cdot \tilde{\text{S}}$  and  $\tilde{\text{LS}}'$  in the form

$$\begin{aligned} \hat{W}_{\text{LS}}^{(\text{odd})}(\mathbf{q}, \mathbf{h}, \mathbf{h}', \boldsymbol{\sigma}, \boldsymbol{\sigma}'; \omega) &= \frac{\tilde{V}_{\text{p-h}}^{(\text{LS})}(q)}{1 - \frac{1}{8} \chi_0(q; \omega) \chi_0^{(\perp)}(q; \omega) [\tilde{V}_{\text{p-h}}^{(\text{LS})}(q)]^2} \left[ \tilde{\text{L}} \cdot \tilde{\text{S}} - \frac{1}{2} \tilde{\text{LS}}' \right] + \frac{1}{2} \frac{\tilde{V}_{\text{p-h}}^{(\text{LS})}(q)}{1 - \frac{1}{4} \chi_0(q; \omega) \chi_0^{(\perp)}(q; \omega) [\tilde{V}_{\text{p-h}}^{(\text{LS})}(q)]^2} \tilde{\text{LS}}' \\ &\equiv \tilde{W}_{\text{LS}}^{(\text{LS})}(q; \omega) \tilde{\text{L}} \cdot \tilde{\text{S}} + \tilde{W}_{\text{LS}}^{(\text{LS}')}(q; \omega) \tilde{\text{LS}}'. \end{aligned} \quad (\text{A10})$$

## 2. Chain-diagram summation for the full operator structure

An important relationship to obtain the chain-diagram summation of all operators is

$$[\{\mathbb{1}, \hat{T}\} * \chi_0 * \{\tilde{\text{L}} \cdot \tilde{\text{S}}, \tilde{\text{LS}}'\} * \chi_0 * \{\mathbb{1}, \hat{T}\}] = 0, \quad (\text{A11})$$

from which we conclude

$$[\{\mathbb{1}, \hat{T}\} * \chi_0 * \hat{W}_{\text{LS}}^{(\text{odd})} * \chi_0 * \{\mathbb{1}, \hat{T}\}] = 0. \quad (\text{A12})$$

That is, no terms with an odd number of  $\hat{V}_{\text{p-h}}^{(\text{LS})}(\mathbf{q})$  operators can exist between  $\mathbb{1}$  and  $\hat{T}$ . Chains that are combinations of  $\hat{V}_{\text{p-h}}^{(\text{c})}(q)$  and  $\hat{V}_{\text{p-h}}^{(\text{T})}(q)$  and all possible even-order  $\hat{V}_{\text{p-h}}^{(\text{LS})}(\mathbf{q})$  are then easily summed by using the orthogonality relations (2.15).

For a compact representation, redefine the particle-hole interactions

$$\tilde{V}_{\text{p-h}}^{(\text{c})}(q) \rightarrow \tilde{V}_{\text{p-h}}^{(\text{c})}(q; \omega) \equiv \tilde{V}_{\text{p-h}}^{(\text{c})}(q) + \frac{1}{4} \chi_0^{(\perp)}(q; \omega) [\tilde{V}_{\text{p-h}}^{(\text{LS})}(q)]^2, \quad (\text{A13a})$$

$$\tilde{V}_{\text{p-h}}^{(\text{T})}(q) \rightarrow \tilde{V}_{\text{p-h}}^{(\text{T})}(q; \omega) \equiv \tilde{V}_{\text{p-h}}^{(\text{T})}(q) + \frac{1}{8} \chi_0^{(\perp)}(q; \omega) [\tilde{V}_{\text{p-h}}^{(\text{LS})}(q)]^2, \quad (\text{A13b})$$

which are now energy dependent. The longitudinal interaction,  $\tilde{V}_{\text{p-h}}^{(\text{L})}(q)$ , is unchanged. That way, the contribution of all terms containing only subchains of an even number of spin-orbit operators in the  $\hat{Q}_\alpha \in \{\mathbb{1}, \hat{L}, \hat{T}\}$  channels can be written as

$$\hat{W}^{\text{even}}(\mathbf{q}, \mathbf{h}, \mathbf{h}', \boldsymbol{\sigma}, \boldsymbol{\sigma}'; \omega) = \sum_{\alpha} \tilde{W}^{(\text{even}, \alpha)}(q; \omega) \hat{Q}_\alpha, \quad (\text{A14})$$

where all channels of  $\tilde{W}^{(\text{even}, \alpha)}(q; \omega)$  are given by Eqs. (2.10) with  $\tilde{V}_{\text{p-h}}^{(\alpha)}(q)$  replaced by  $\tilde{V}_{\text{p-h}}^{(\alpha)}(q; \omega)$ , defined in Eqs. (2.17a) and (2.17b) for  $\hat{Q}_\alpha \in \{\mathbb{1}, \hat{T}\}$  channels. Finally, we need to include those terms in the chains that contain odd-order chains of  $\hat{V}_{\text{p-h}}^{(\text{LS})}(\mathbf{q})$ ,

as well as  $\hat{Q}_7$  and  $\hat{Q}_9$  channels in (A6). The total effective interaction then has the form

$$\hat{W} = \hat{W}^{(\text{even})} + \hat{W}_{\text{LS}}^{(\text{odd})} + \sum_{\alpha \in \{c, T\}} [\tilde{V}_{\text{p-h}}^{(\alpha)} + \tilde{V}_{\text{p-h}}^{(\alpha)} \chi_0 \tilde{W}^{(\text{even}, \alpha)}] \hat{W}^{(1 \text{ odd}, \alpha)} + \sum_{\alpha \in \{c, T\}} [\tilde{V}_{\text{p-h}}^{(\alpha)} + [\tilde{V}_{\text{p-h}}^{(\alpha)}]^2 \chi_0 + [\tilde{V}_{\text{p-h}}^{(\alpha)}]^2 \chi_0^2 \tilde{W}^{(\text{even}, \alpha)}] \hat{W}^{(2 \text{ odd}, \alpha)}, \quad (\text{A15})$$

where

$$\hat{W}^{(1 \text{ odd}, \alpha)} = [\hat{W}^{(\text{odd})} * \chi_0 * \hat{Q}_\alpha + \hat{Q}_\alpha * \chi_0 * \hat{W}^{(\text{odd})}] \quad (\text{A16})$$

represents chaining with  $\hat{W}^{(\text{odd})}$  on either side, and

$$\hat{W}^{(2 \text{ odd}, \alpha)} = [\hat{W}^{(\text{odd})} * \chi_0 * \hat{Q}_\alpha * \chi_0 * \hat{W}^{(\text{odd})}] \quad (\text{A17})$$

represents chaining with  $\hat{W}^{(\text{odd})}$  on both sides.

Working out these relationships using Eqs. (A9) we end up with the compact representation of the remaining contributions to the effective interaction:

$$\tilde{W}^{(7)}(q; \omega) = \frac{1}{4} \frac{[\tilde{V}_{\text{p-h}}^{(\text{LS})}(q)]^2 \chi_0(q; \omega)}{1 - \chi_0(q; \omega) \tilde{V}_{\text{p-h}}^{(c)}(q; \omega)}, \quad (\text{A18a})$$

$$\tilde{W}^{(9)}(q; \omega) = \frac{1}{8} \frac{[\tilde{V}_{\text{p-h}}^{(\text{LS})}(q)]^2 \chi_0(q; \omega)}{1 - \chi_0(q; \omega) \tilde{V}_{\text{p-h}}^{(T)}(q; \omega)}, \quad (\text{A18b})$$

$$\tilde{W}^{(\text{LS})}(q; \omega) = \frac{\tilde{V}_{\text{p-h}}^{(\text{LS})}(q)}{1 - \chi_0(q; \omega) \tilde{V}_{\text{p-h}}^{(T)}(q; \omega)}, \quad (\text{A18c})$$

$$\tilde{W}^{(\text{LS}')} (q; \omega) = \frac{\tilde{V}_{\text{p-h}}^{(\text{LS})}(q) \chi_0(q; \omega) V_{\text{p-h}}^{(c)}(q; \omega)}{1 - \chi_0(q; \omega) \tilde{V}_{\text{p-h}}^{(c)}(q; \omega)} - \frac{\tilde{V}_{\text{p-h}}^{(\text{LS})}(q) \chi_0(q; \omega) V_{\text{p-h}}^{(T)}(q; \omega)}{1 - \chi_0(q; \omega) \tilde{V}_{\text{p-h}}^{(T)}(q; \omega)}. \quad (\text{A18d})$$

## APPENDIX B: CALCULATION OF $\chi_0^{(\perp)}(q; \omega)$

In this section, we show details for the calculation of

$$\chi_0^{(\perp)}(q; \omega) = -\frac{1}{N} \sum_{\mathbf{h}} n(\mathbf{h}) \bar{n}(\mathbf{h} - \mathbf{q}) \chi_0(\mathbf{q}, \mathbf{h}; \omega) (\hat{\mathbf{q}} \times \mathbf{h}_F)^2. \quad (\text{B1})$$

We assume in this Appendix that all wave numbers are given in units of the Fermi wave number  $k_F$  and all energies in units of the Fermi energy  $e_F$ . Also, let  $x \equiv \hbar\omega/e_F$ . Note that we use a slightly different convention as usual [72] in the sense that the Lindhard function has the dimension of an inverse energy. The integrals are done in cylindrical coordinates with  $\mathbf{q}$  pointing in the  $z$  direction. To calculate  $\chi_0^{(\perp)}(q; \omega)$ , use

$$|\hat{\mathbf{q}} \times \mathbf{h}_F|^2 = \hbar^2 \sin^2 \theta = \hbar^2 - z^2 \equiv \rho^2.$$

Then we have

$$\begin{aligned} \chi_0^{(\perp)}(q; \omega) &= \int \frac{d^3k}{V_F} n(k) \bar{n}(\mathbf{k} + \mathbf{q}) \frac{2\rho^2(q^2 + 2qz)}{(x + i\eta)^2 - (q^2 + 2qz)^2} \\ &= \frac{3}{2} \left[ \int_{-q/2}^1 dz \int_0^{\sqrt{1-z^2}} \rho^3 d\rho - \int_{-q/2}^{1-q} dz \int_0^{\sqrt{1-(z+q)^2}} \rho^3 d\rho \right] \frac{2(q^2 + 2qz)}{(x + i\eta)^2 - (q^2 + 2qz)^2} \\ &= \frac{3}{8} \left[ \int_{-q/2}^1 dz (1 - z^2)^2 - \int_{-q/2}^{1-q} dz (1 - (z + q)^2)^2 \right] \times \frac{2(q^2 + 2qz)}{(x + i\eta)^2 - (q^2 + 2qz)^2}. \end{aligned} \quad (\text{B2})$$

We get for the real part

$$\text{Re } \chi_0^{(\perp)}(q; \omega) = \frac{3q^2}{32} - \frac{5}{8} + \frac{9}{32} \frac{x^2}{q^2} - \frac{3}{256q^5} \left[ ((q^2 - x)^2 - 4q^2)^2 \ln \left| \frac{x - q^2 - 2q}{x - q^2 + 2q} \right| - ((q^2 + x)^2 - 4q^2)^2 \ln \left| \frac{x + q^2 - 2q}{x + q^2 + 2q} \right| \right]. \quad (\text{B3})$$



We obtain for the imaginary part for  $q \leq 2$

$$\text{Im } \chi_0^{(\perp)}(q; \omega) = \begin{cases} \frac{3\pi x}{32q^3}(q^4 - 4q^2 + x^2) & \text{for } 0 \leq x \leq 2q - q^2, \\ -\frac{3\pi}{256q^5}[(q^2 - x)^2 - 4q^2]^2 & \text{for } 2q - q^2 \leq x \leq q^2 + 2q, \\ 0 & \text{for } q^2 + 2q < x \end{cases} \quad (\text{B4})$$

and for  $q > 2$

$$\text{Im } \chi_0^{(\perp)}(q; \omega) = \begin{cases} -\frac{3\pi}{256q^5}[(q^2 - x)^2 - 4q^2]^2 & \text{for } q^2 - 2q \leq x \leq q^2 + 2q, \\ 0 & \text{elsewhere.} \end{cases} \quad (\text{B5})$$

The frequency integrations in Eqs. (2.33) and (2.48) are best performed by Wick rotation along the imaginary  $\omega$  axis. For that purpose we need the transverse Lindhard function on the imaginary  $\omega$  axis:

$$\begin{aligned} \chi_0^{(\perp)}(q, i\omega) = & \frac{3}{32}q^2 - \frac{5}{8} - \frac{9}{32}\frac{x^2}{q^2} + \frac{3}{32q^3}[x^2 + q^2(4 - q^2)] \arctan[4qx, x^2 + q^2(q^2 - 4)] \\ & + \frac{3}{256q^5}\{[x^2 + q^2(4 - q^2)]^2 - 4x^2q^4\} \ln \left| \frac{(q - 2)^2 + x^2}{(q + 2)^2 + x^2} \right|. \end{aligned} \quad (\text{B6})$$

- 
- [1] R. V. Reid, Jr., *Ann. Phys. (NY)* **50**, 411 (1968).  
 [2] H. A. Bethe and M. B. Johnson, *Nucl. Phys. A* **230**, 1 (1974).  
 [3] B. D. Day, *Phys. Rev. C* **24**, 1203 (1981).  
 [4] R. B. Wiringa, V. G. J. Stoks, and R. Schiavilla, *Phys. Rev. C* **51**, 38 (1995).  
 [5] R. B. Wiringa, R. A. Smith, and T. L. Ainsworth, *Phys. Rev. C* **29**, 1207 (1984).  
 [6] E. Krotscheck and J. Wang, *Phys. Rev. C* **101**, 065804 (2020).  
 [7] E. Krotscheck and J. Wang, *Phys. Rev. C* **102**, 064305 (2020).  
 [8] I. Bombaci, A. Fabrocini, A. Polls, and I. Vidana, *Phys. Lett. B* **609**, 232 (2005).  
 [9] M. Modarres and A. Tafrihi, *Nucl. Phys. A* **941**, 212 (2015).  
 [10] A. Tafrihi and M. Modarres, *Nucl. Phys. A* **958**, 25 (2017).  
 [11] A. Tafrihi, *Ann. Phys. (NY)* **392**, 12 (2018).  
 [12] K. A. Brueckner, C. A. Levinson, and H. M. Mahmoud, *Phys. Rev.* **95**, 217 (1954).  
 [13] K. A. Brueckner, *Phys. Rev.* **100**, 36 (1955).  
 [14] K. A. Brueckner, *Phys. Rev.* **97**, 1353 (1955).  
 [15] K. A. Brueckner, in *Lecture Notes of the 1957 Les Houches Summer School*, edited by C. DeWitt and P. Nozières (Dunod, Paris, 1959), pp. 47–241.  
 [16] H. A. Bethe and J. Goldstone, *Proc. R. Soc. London, Ser. A* **238**, 551 (1957).  
 [17] J. Goldstone, *Proc. R. Soc. London, Ser. A* **239**, 267 (1957).  
 [18] D. Pines and P. Nozières, *The Theory of Quantum Liquids* (Benjamin, New York, 1966), Vol. I.  
 [19] D. J. Thouless, *The Quantum Mechanics of Many-Body Systems*, 2nd ed. (Academic, New York, 1972).  
 [20] G. Baym and L. P. Kadanoff, *Phys. Rev.* **124**, 287 (1961).  
 [21] R. Jastrow, *Phys. Rev.* **98**, 1479 (1955).  
 [22] E. Feenberg, *Theory of Quantum Fluids* (Academic, New York, 1969).  
 [23] C.-H. Yang and J. W. Clark, *Nucl. Phys. A* **174**, 49 (1971).  
 [24] E. Krotscheck and J. W. Clark, *Nucl. Phys. A* **333**, 77 (1980).  
 [25] S. Fantoni, *Nucl. Phys. A* **363**, 381 (1981).  
 [26] A. Fabrocini, S. Fantoni, A. Y. Illarionov, and K. E. Schmidt, *Phys. Rev. Lett.* **95**, 192501 (2005).  
 [27] A. Fabrocini, S. Fantoni, A. Y. Illarionov, and K. E. Schmidt, *Nucl. Phys. A* **803**, 137 (2008).  
 [28] H.-H. Fan and E. Krotscheck, *Phys. Rep.* **823**, 1 (2019).  
 [29] E. Krotscheck and J. Wang, *Phys. Rev. C* **103**, 035808 (2021).  
 [30] H. K. Sim, C.-W. Woo, and J. R. Buchler, *Phys. Rev. A* **2**, 2024 (1970).  
 [31] A. D. Jackson, A. Lande, and R. A. Smith, *Phys. Rep.* **86**, 55 (1982).  
 [32] A. D. Jackson, A. Lande, and R. A. Smith, *Phys. Rev. Lett.* **54**, 1469 (1985).  
 [33] E. Krotscheck, R. A. Smith, and A. D. Jackson, *Phys. Rev. A* **33**, 3535 (1986).  
 [34] S. Fantoni and S. Rosati, *Nuovo Cimento A* **43**, 413 (1978).  
 [35] V. R. Pandharipande and R. B. Wiringa, *Rev. Mod. Phys.* **51**, 821 (1979).  
 [36] E. Krotscheck, *Nucl. Phys. A* **482**, 617 (1988).  
 [37] R. A. Smith and A. D. Jackson, *Nucl. Phys. A* **476**, 448 (1988).  
 [38] L. D. Landau, *Sov. Phys. JETP* **3**, 920 (1957).  
 [39] L. D. Landau, *Sov. Phys. JETP* **5**, 101 (1957).  
 [40] G. Baym and C. Pethick, *Landau Fermi Liquid Theory* (Wiley, New York, 1991).  
 [41] C. H. Aldrich III and D. Pines, *J. Low Temp. Phys.* **31**, 689 (1978).  
 [42] B. L. Friman and E. M. Nyman, *Nucl. Phys. A* **302**, 365 (1978).  
 [43] W. Weise, *Nucl. Phys. A* **278**, 402 (1977).  
 [44] A. Pastore, D. Davesne, and J. Navarro, *J. Phys. G* **41**, 055103 (2014).  
 [45] A. Pastore, D. Davesne, and J. Navarro, *Phys. Rep.* **563**, 1 (2015).  
 [46] C. García-Recio, J. Navarro, V. Nguyen, and L. L. Salcedo, *Ann. Phys. (NY)* **214**, 293 (1992).  
 [47] E. S. Hernandez, J. Navarro, and A. Polls, *Nucl. Phys. A* **627**, 460 (1997).  
 [48] E. S. Hernandez, J. Navarro, and A. Polls, *Nucl. Phys. A* **658**, 327 (1999).  
 [49] D. Davesne, M. Martini, K. Bennaceur, and J. Meyer, *Phys. Rev. C* **80**, 024314 (2009).

- [50] D. Davesne, M. Martini, K. Bennaceur, and J. Meyer, *Phys. Rev. C* **84**, 059904(E) (2011).
- [51] D. Davesne, A. Pastore, and J. Navarro, *Phys. Rev. C* **89**, 044302 (2014).
- [52] D. Davesne, A. Pastore, and J. Navarro, *Phys. Rev. C* **100**, 064301 (2019).
- [53] W. Alberico, M. Ericson, and A. Molinari, *Nucl. Phys. A* **379**, 429 (1982).
- [54] D. Pines, K. F. Quader, and J. Wambach, *Nucl. Phys. A* **477**, 365 (1988).
- [55] D. Pines and D. Bohm, *Phys. Rev.* **82**, 625 (1951).
- [56] D. Pines and D. Bohm, *Phys. Rev.* **85**, 338 (1952).
- [57] J. Sawicki, *Phys. Rev.* **126**, 2231 (1962).
- [58] C. Yannouleas, M. Dworzecka, and J. J. Griffin, *Nucl. Phys. A* **397**, 239 (1983).
- [59] C. Yannouleas, *Phys. Rev. C* **35**, 1159 (1987).
- [60] J. Wambach, *Rep. Prog. Phys.* **51**, 989 (1988).
- [61] P. Papakonstantinou and R. Roth, *Phys. Rev. C* **81**, 024317 (2010).
- [62] H. M. Böhm, R. Holler, E. Krotscheck, and M. Panholzer, *Phys. Rev. B* **82**, 224505 (2010).
- [63] H. Godfrin, M. Meschke, H.-J. Lauter, A. Sultan, H. M. Böhm, E. Krotscheck, and M. Panholzer, *Nature (London)* **483**, 576 (2012).
- [64] C. E. Campbell, E. Krotscheck, and T. Lichtenegger, *Phys. Rev. B* **91**, 184510 (2015).
- [65] K. Beauvois, C. E. Campbell, J. Dawidowski, B. Fåk, H. Godfrin, E. Krotscheck, H.-J. Lauter, T. Lichtenegger, J. Ollivier, and A. Sultan, *Phys. Rev. B* **94**, 024504 (2016).
- [66] E. Krotscheck and T. Lichtenegger, *J. Low Temp. Phys.* **178**, 61 (2015).
- [67] A. D. Jackson, A. Lande, R. W. Guitink, and R. A. Smith, *Phys. Rev. B* **31**, 403 (1985).
- [68] J. W. Clark, in *Progress in Particle and Nuclear Physics*, edited by D. H. Wilkinson (Pergamon Press Ltd., Oxford, 1979), Vol. 2, pp. 89–199.
- [69] E. Krotscheck, *J. Low Temp. Phys.* **119**, 103 (2000).
- [70] B. L. Scott and S. A. Moszkowski, *Nucl. Phys.* **29**, 665 (1962).
- [71] J. C. Owen, R. F. Bishop, and J. M. Irvine, *Nucl. Phys. A* **274**, 108 (1976).
- [72] A. L. Fetter and J. D. Walecka, *Quantum Theory of Many-Particle Systems* (McGraw-Hill, New York, 1971).
- [73] E. Krotscheck, *Phys. Rev. A* **26**, 3536 (1982).
- [74] A. Dellafiore and F. Matera, *Phys. Rev. C* **40**, 960 (1989).
- [75] G. Ripka, *Nucl. Phys. A* **314**, 115 (1979).
- [76] E. Krotscheck, *Phys. Rev. A* **15**, 397 (1977).
- [77] H.-H. Fan, E. Krotscheck, and J. W. Clark, *J. Low Temp. Phys.* **189**, 470 (2017).
- [78] A. D. Jackson and R. A. Smith, *Phys. Rev. A* **36**, 2517 (1987).
- [79] C. E. Campbell, R. Folk, and E. Krotscheck, *J. Low Temp. Phys.* **105**, 13 (1996).
- [80] P. Haensel and A. J. Jerzak, *Acta Phys. Pol. B* **14**, 953 (1983).
- [81] C. H. Aldrich and D. Pines, *J. Low Temp. Phys.* **25**, 677 (1976).
- [82] E. Krotscheck, *Phys. Rev. B* **33**, 3158 (1986).
- [83] N.-H. Kwong, Realistic calculations of excitations in nuclear matter, Ph.D. thesis, California Institute of Technology, 1982 (unpublished).
- [84] O. Benhar and N. Farina, *Phys. Lett. B* **680**, 305 (2009).
- [85] A. Lovato, C. Losa, and O. Benhar, *Nucl. Phys. A* **901**, 22 (2013).